Title: Experimental evolution of gene essentiality in bacteria

Authors: Liang Bao[1, *], Zan Zhu[1], Ahmed Ismail[1], Bin Zhu[2], Vysakh Anandan[1], Marvin Whiteley[3], Todd Kitten[1], Ping Xu[1, *]

Affiliations:
1, Department of Oral and Craniofacial Molecular Biology, Philips Institute for Oral Health Research, School of Dentistry, Virginia Commonwealth University, Virginia, USA.
2, Massey Cancer Center, Virginia Commonwealth University, Virginia, USA.
3, School of Biological Sciences, Center for Microbial Dynamics and Infection, Georgia Institute of Technology, Georgia, USA.

Correspondence:

pxu@vcu.edu (P.X.), baol@vcu.edu (L.B.)

Summary

Essential gene products carry out fundamental cellular activities in interaction with other components. However, the lack of essential gene mutants and appropriate methodologies to link essential gene functions with their partners poses significant challenges. Here, we have generated deletion mutants in 32 genes previously identified as essential, with 23 mutants showing extremely slow growth in the SK36 strain of *Streptococcus sanguinis*. Whole-genome sequencing of 243 independently evolved populations of these mutants has identified >1000 spontaneous suppressor mutations in experimental evolution, many of which define new gene and pathway relationships, such as F1Fo-ATPase/V1Vo-ATPase/TrkA1-H1. Patterns of spontaneous mutations occurring in essential gene mutants differed from those found in wildtype. While gene duplications occurred rarely and appeared most often at later stages of evolution, substitutions, deletions, and insertions were prevalent in evolved populations. These essential gene deletion mutants and spontaneous mutations fixed in the mutant populations during evolution establish a foundation for understanding gene essentiality and the interaction of essential genes in networks.

Keywords

Gene essentiality; Experimental evolution; Spontaneous mutations; Whole-genome sequencing; *Streptococcus*; F1Fo-ATPase/V1Vo-ATPase/TrkA1-H1 gene pathway.

Introduction

All living organisms require certain physical properties and biochemical capacities encoded by "essential" genes to sustain basic cellular activities. Essential genes are indispensable for an

organism to survive or reproduce, and their essentiality is highly dependent on the environment in which the organism lives. [1,2] *In vivo*, essential gene products carry out these tasks by interacting with other components. Therefore, the essentiality of genes can also depend on the genetic context provided by the additional genes present. [2-4] Relationships may be characterized by negative epistasis when the essentiality of a gene is dependent on the absence or impairment of another gene's function, such as synthetic lethality [3,5] or positive epistasis interactions, where an individual with two genes mutated is fitter than a strain possessing a mutant version of only one of the two genes. [3,6,7] In contrast to binary classification, it is increasingly acknowledged that essential genes exhibit a quantitative spectrum, displaying a gradient of essentiality [2] and a conditional nature. [8] For some essential genes, under optimal controlled conditions, deletion can still result in viable, albeit severely compromised individuals. [9,10] The loss of essential genes produces intense selective pressure for the fixation of genomic suppressor mutations in the descendants of the original mutants during subsequent generations, including aneuploidy of chromosomes. [9,10] Furthermore, essential genes can lose their essentiality during long-term evolution and acquire novel functions. [11-13] For instance, unlike the essential characteristics of the critical cell cycle regulator *CDK1* in yeasts and animals, [14] plant PSTAIRE-type cyclin-dependent kinases, known as *CDKAs* (plant homologs of *CDK1*), play a role in environmental responses that is independent of the cell cycle, [11] likely after the acquisition of the plant-specific cyclin-dependent kinases, *CDKBs*. [15]

Identifying genes that interact with essential genes can produce many potential benefits, both from a theoretical perspective, such as understanding the basic principles of cellular life,[16,17] and from a practical standpoint, such as addressing various challenges in synthetic biology [18] and combating drug resistance of infectious diseases. [17] Experimental evolution or laboratory evolution imposes a natural selective pressure on a population to redirect the evolution towards fitness-improving phenotypes in a controlled laboratory setting. [9,10,19-25] This methodology has been applied to identify spontaneous mutations associated with fitness-improving phenotypes, such as multicellularity, [19] novel metabolic capacity, [20] restoration of flagellar mobility,[26] and fitness of minimal cells. [21] Recently, experimental evolution using mutants deleted of essential genes in the yeast *Saccharomyces cerevisiae* revealed a rapid growth phenotype after passages. [9,10] However, aneuploidy of chromosomes was prevalent among evolved populations deleted of essential genes, which hindered the identification of causal suppressors. [9,10] Here, we have established a transformation system to obtain numerous essential gene knockout mutants, including *obgE*, *pfkA*, and subunits of F1Fo-ATPase that have been identified as essential in most bacterial species, including all species of *Streptococcus* examined (http://www.essentialgene.org/), and performed experimental evolution of mutants deleted for essential genes using a *Streptococcus* bacterium as our model. After allowing for short-term adaptation, we have identified >1000 spontaneous suppressor mutations in 243 evolved populations deleted of essential genes, most of which are substitutions, deletions, and insertions. This feature enabled us to map virtually all mutations to distinct genomic segments of individual ORFs or intergenic regions. For comparison, we also evaluated the twelve mutations that arose in six evolved populations in the wild-type (WT) cells. The mutations that occurred in essential gene mutants displayed several characteristics that distinguished them from those that evolved in WT cells during short-term evolution.

Results

86
87 **Isolating essential gene mutants and analysis of short-term evolution**
88
89 The genome of *Streptococcus sanguinis* SK36 comprises over 2000 ORFs, [27] of which 218 have
90 been experimentally identified as essential for the organism's survival when cells are grown on a
91 rich medium—brain heart infusion (BHI) broth or plates—under microaerobic conditions. [1] To
92 isolate viable essential-gene deletion mutants, we have modified our transformation procedure to
93 minimize stress (see Materials and Methods). Although we still employed homologous
94 recombination (Fig. 1a and Supplementary Fig.1a), we replaced our conventional 1-hour aerobic
95 transformation with an anaerobic incubation and a duration of up to 24 hours. [1] Additionally, we
96 optimized the selection conditions by covering the transformants with a thin layer of agar
97 medium and extending the selection period for the transformants to four to six days, all
98 conducted under anaerobic conditions. (See Materials and Methods.)
99
100 Using this procedure, we observed an interesting phenomenon. Specifically, for 23 of the
101 essential genes, the transformants produced two types of colonies: large and small (Fig. 1B, and
102 Supplementary Fig.2a). As expected, genotyping of the small colonies revealed a complete
103 replacement of the corresponding ORF with a kanamycin resistance (*kan*) gene (Supplementary
104 Fig.1b). In contrast, genotyping of the large colonies showed that some mutants displayed a
105 "double band" genotype due to duplication of the target gene prior to the replacement of one
106 copy by the *kan* gene (Supplementary Fig.1c, Supplemental Table 1). This finding suggests that
107 *S. sanguinis* SK36 regularly undergoes gene duplications, particularly between two copies of a
108 multi-copy gene or locus, such as the rRNA operons. Alternatively, some large colonies lacked a
109 *kan* gene, but contained point mutations in different genes, with the majority of isolates acquiring
110 mutations in translational machinery genes that may confer resistance to kanamycin, [28] such as
111 *fusA, rpsL* or *rplF* (Supplemental Table 1). Among fifty-four large colonies genotyped, fifteen
112 showed the double-band genotype. The remaining thirty-nine did not contain the *kan* gene, but
113 thirty-eight, or 97.4% contained mutations in *fusA, rpsL* or *rplF* (Supplemental Table 1). In
114 contrast, for nine essential genes, the deletion mutants exhibited robust growth (Supplementary
115 Fig.2b). These nine genes included *nrdE, nrdF, nrdH,* and *nrdI* which were previously reported
116 as non-essential under anaerobic conditions but essential in the presence of O_2, [29] along with
117 *rexB* for ATP-dependent nuclease subunit B, *rpsA* for 30S ribosomal protein S1, *pdf* for peptide
118 deformylase, and *g6pD* for glucose-6-phosphate dehydrogenase (Supplementary Fig.2b).
119
120 We, therefore, directed our attention to the twenty-three essential genes that, when deleted, led to
121 severe growth defects in the resultant mutants. These twenty-three genes encoding components
122 of diverse pathways, include the eight subunit genes encoding the F1Fo-ATPase (*uncE*, *uncB*,
123 *uncF*, *uncH*, *uncA*, *uncG*, *uncD*, and *uncC)*; *ftsX,* encoding a permease-like cell division protein;
124 five *fab* genes (*fabH*, *fabK*, *fabG*, *fabF*, and *fabZ*) that are involved in Type-II fatty acid
125 synthesis (FAS II); two ribosomal protein genes (*rplV* and *rpmH*); two GTPase genes (*obgE* and
126 *yihA*); *yqeG,* encoding a YqeG-family phosphatase; *pfkA*, encoding 6-phosphofructokinase,
127 involved in glycolysis; *pngM*, encoding phosphoglucomutase; *dpcK* (also called *coaE*), encoding
128 diphospho-CoA kinase, involved in CoA synthesis; and *dnaK*, encoding a heat shock protein
129 chaperone. These genes are widely distributed and are essential in various genera and species
130 (http://www.essentialgene.org/). [30] In total, we have created 23 essential gene mutants, each with
131 an individual gene deletion, along with one mutant deleted for the entire *f1fo* region encoding the

132 eight F1Fo-ATPase subunits, which we have named Δ*f1fo* (Supplementary Fig.1 and S2a.1-a.2).
133 Although the deletion mutants of the 23 genes were initially generated under anaerobic condition
134 in this study, we have confirmed the viability of mutants under both anaerobic (Supplementary
135 Fig.3a) and microaerobic (Supplementary Fig.3b) conditions, as utilized previously for
136 identification of essential genes in *S. sanguinis* SK36. [1]
137
138 In order to study the evolution of gene essentiality, we conducted passage experiments using
139 multiple independently evolved populations of the 24 essential gene mutants. To form a
140 population, we selected three to five colonies from the selection medium, combined them into a
141 single inoculum, and subjected them to passage in BHI by 1:20 serial transfer. To ensure a
142 comparable number of generations, we closely monitored the growth of mutants during each
143 passage. We proceeded to the following passage only when the cell cultures had reached an
144 OD_{600} within the range of 0.1-0.5. As a control, WT cells, which reached an OD_{600} of
145 approximately 1.0 within 24 hours of growth, or 2-10 times more cells compared to the mutants
146 in each passage, were passaged daily for a total of nine times. This method was applied to
147 maintain consistency throughout the experimental process (Fig. 1c, Supplementary Fig.3c, and
148 Supplemental Table 2). While all mutants exhibited significant growth defects compared to WT,
149 we observed variations in their growth phenotypes. Notably, mutants lacking *pfkA, fabK, fabG,*
150 *fabF*, and *fabZ* displayed the most severe growth defects. In contrast, the growth of others,
151 including another *fab* mutant, *fabH,* was less severe, as evidenced by the OD_{600} measurements of
152 the evolved mutants (Fig. 1c and Supplementary Fig.3c, Supplemental Table 2). In our passage
153 experiments, we observed that the mutants in passage 6 (P6, "P" for passage) exhibited enhanced
154 fitness compared to those in early passages. For example, the time required for cultures to reach
155 an OD_{600} of 0.1-0.5 in P0 compared to P6 (Fig. 1c, Supplemental Table 3) indicated faster
156 growth at P6, reflecting improved fitness.
157
158 **Identification of suppressor loci in evolved populations deleted of essential genes and in**
159 **WT**
160
161 To identify suppressor mutations in the evolved populations deleted of essential genes, we
162 performed whole-genome sequencing at P6. Specifically, we sequenced between two and
163 twenty-five independently evolved populations for each of the twenty-four essential gene
164 mutants, resulting in a total of 243 populations (Fig. 2a and Supplemental Table 4). As controls,
165 we also sequenced six populations of WT, which were generated by aliquoting into six separate
166 tubes and passaging nine times, as well as the original WT (Fig. 2a and Supplemental Table 4).
167
168 We first considered mutations related to duplications of genes other than the essential gene
169 targeted for mutagenesis. Of the 243 evolved mutant populations, we found that twelve (4.9%)
170 displayed gene duplications of various sizes, ranging from 10 kb to 310 kb. By comparison, none
171 of the six evolved WT populations in P9 nor the original parental WT contained a gene
172 duplication (Supplementary Fig.4a). For the twelve evolved mutant populations with gene
173 duplications, two were from Δ*f1fo* (*#107* and *#109*) (Fig. 2a and Supplementary Fig.4b), one
174 from Δ*uncE* (*#2*) (Supplementary Fig.4c), one from Δ*uncH* (*#7*) (Fig. 2c), three from Δ*fabH* (#4,
175 #6 and #14) (Fig. 2d and Supplementary Fig.4d and S4e), one from Δ*fabF (#4)* (Fig. 2e), two
176 from Δ*fabZ* (*#1 and #3*) (Fig. 2f and 2c), one from Δ*obgE* (*#5*) (Fig. 2h) and one from Δ*dpcK*
177 (*#17*) (Fig. 2i). The duplicated regions found in populations of Δ*f1fo,* Δ*uncE,* Δ*uncH,* Δ*fabH* and

178 Δ*fabF* mutants encompassed the same ~103 kb region (coordinate: 22,738-125,834) that is
179 flanked by two directly repeated rRNA operons (Fig. 2b-e). The above-duplicated region of ~103
180 kb contains 113 ORFs, including nine ORFs encoding the entire V1Vo-ATPase operon that is
181 related to the proton pump function of F1Fo-ATPase, [31] one ORF encoding acyl carrier protein
182 and one ORF encoding acyltransferase that is related to lipid biosynthesis. [32] The duplicated
183 region found in Δ*fabZ#1* spans approximately 143 kb (coordinate: 1,053,488-1,197,391). The
184 10.1-kb duplication in Δ*fabZ#3* (coordinate: 1,093,824-1,103,958) is within the duplicated 143
185 kb in Δ*fabZ#1.* This 10.1-kb region contains ten ORFs, including one ORF annotated as acyl-
186 acyl carrier protein thioesterase, which catalyzes the terminal reaction of fatty acid biosynthesis
187 (Jing, et al., 2011). In the case of Δ*obgE#5*, a 37-kb duplication is present (coordinate:
188 1,775,394-1,812,805), encompassing thirty ORFs, including one ORF encoding der GTPase. In
189 Δ*dpcK#17,* a ~310-kb duplication occurred (coordinate: 385,678-697,581), encompassing 305
190 ORFs. The flanking sequences of the duplicated regions in Δ*fabZ#1,* Δ*fabZ#3,* Δ*obgE#5* and
191 Δ*dpcK#17* possessed no notable repeated sequences.
192
193 Next, we assessed substitutions, deletions, and insertions of less than 10 kb in the evolved
194 populations. The genome of *S. sanguinis* can be divided into 4,283 segments—2,340 ORFs and
195 1,943 intergenic regions (Supplemental Table 5). [33] We defined a segment as mutated if any
196 mutation within that segment was present in at least 30% of the sequence reads (see Materials
197 and Methods section). We selected 30% as the threshold based on our finding that confirmed
198 suppressor mutations, such as *trkA1-H1*, ranged from 34.8% to 100% in the evolved Δ*f1fo*
199 populations in P6 (Fig. 4d and Supplemental Table 4). There were six mutations (two
200 substitution mutations and four deletion mutations from the six evolved populations), where two
201 to four ORFs were affected by each mutation. For example, the C to T (at coordinate 1,313,563)
202 mutation in Δ*fabF#10* caused amino substitutions of two overlapping ORFs encoding two
203 hypothetical proteins (Supplemental Table 4). The remaining mutations fell within single
204 segments of ORFs or intergenic regions. In total, we detected 1,272 mutated segments
205 (Supplemental Table 4), with 1,260 from evolved populations lacking essential genes and twelve
206 from the evolved WT populations (Supplemental Table 4). Our analysis revealed that each of the
207 243 (100%) evolved mutant populations contained at least one mutated segment, with the
208 majority containing from 2 to 10 (Fig. 2j and Supplemental Table 4-6). In contrast, among the
209 six evolved WT populations, four had at least one segment containing a mutation in at least 30%
210 of the sequence reads, while the remaining two, as well as the parental WT population, had none
211 (Fig. 2j and Supplemental Table 4). Furthermore, when we set the threshold to 50%, 241 evolved
212 mutant populations, or 99.2%, had mutated segments, whereas none of the six evolved WT
213 populations contained mutated segments (Fig. 2k and Supplemental Table 7) ($\chi 2$=154.69, df=1,
214 n=249 populations, p=2.2e-16).
215
216 We then analyzed the presence of mutated segments belonging to essential ORFs (in each case,
217 excluding the ORF that was intentionally deleted in each mutant, as well as the nine
218 conditionally essential genes). We found that suppressor mutations belonging to essential
219 segments were present in at least one evolved population from each essential gene mutant (Fig.
220 2l and Supplemental Table 8-9). In contrast, none of the twelve mutated segments from the
221 evolved WT populations were found to be within an essential ORF (Fig. 2l and Supplemental
222 Table 8-9) ($\chi 2$=5.74, df=1, n=25 groups, p=0.017). To illustrate this further, we compared the
223 frequency of mutated segments in P1 and P6 for two specific cases: mutations of *ftsZ* (an

224 essential segment encoding a structural homolog of tubulin in prokaryotes) in the evolved
225 Δ*f1fo#107* and *uncH* (an essential segment, encoding delta subunit of F1Fo-ATPase) in the
226 evolved Δ*uncC#1*. The *uncH* gene is located 3.9 kb upstream of *uncC*, both of which are within
227 the *f1fo* operon. The evolved Δ*uncC#1* population of P1 did not have any *uncH* mutations using
228 30% as the cutoff, although an *uncH* mutation was present in 12% of the sequence reads
229 (Supplementary Fig.5a-c). In contrast, the Δ*uncC#1* population of P6 contained 86% *uncH*
230 mutation (Supplementary Fig.5d-f) The resultant mutation replaced a 207-bp segment that was
231 51 bp downstream of the *uncH* start codon with an 82-bp fragment, causing early truncation
232 (Supplementary Fig.5g). For the second case, the *ftsZ* gene is located approximately 126 kb
233 upstream of the *f1fo* operon. In the evolved Δ*f1fo#107* population in P1, we did not detect any
234 mutations in the *ftsZ* segment using 30% abundance as cutoff, although 27% of the sequence
235 reads contained a *ftsZ* mutation (Supplementary Fig.5g-h). In comparison, the evolved
236 population of P6 contained 100% mutated *ftsZ*—a 248 bp insertion located 1015 bp downstream
237 of the start codon (Supplementary Fig.5I-J), leading to the truncation of the FtsZ protein
238 (Supplementary Fig.5k). These findings demonstrate an increase of mutated essential segments
239 in the essential gene deletion mutant due to selection during passage.
240
241 Multi-drug resistance across ESKAPE pathogens (i.e., *Enterococcus faecium*, *Staphylococcus*
242 *aureus*, *Klebsiella pneumoniae*, *Acinetobacter baumannii*, *Pseudomonas aeruginosa*, and
243 *Enterobacter spp.*) has been found to be commonly associated with mutations in six genes—
244 namely, *rrs, gyrA*, *gyrB*, *rpoB, rpsL* and *rsmG* (also known as *gidB*). [34] We therefore asked
245 whether mutations in the typical set of multi-drug resistance-associated genes [34] could appear in
246 the evolved populations deleted of essential genes. Apart from the 16S rRNA gene, which is
247 present in four copies (*rrs1* to *rrs4*), *S. sanguinis* has one copy of each of these genes. Among
248 the 243 evolved populations deleted of essential genes, mutations of multi-drug resistance genes
249 were present in *rrs2*, *rpoB*, *gyrB,* and *rspL* in a variety of populations derived from different
250 essential gene mutants, while no mutations were detected in *rrs1*, *rrs3*, *rrs4*, *gyrA* or *rsmG*.
251 Moreover, no mutation was detected within this set of multi-drug resistance-associated genes in
252 the evolved WT populations (Fig. 2m and Supplemental Table 10). These results showed that
253 missense mutations in four of the same genes that promote multi-drug resistance also improve
254 the fitness of mutants deleted of these particular essential genes.
255
256 In summary, compared to the evolved WT populations, mutants deleted for essential genes
257 exclusively evolve gene duplications of greater than 10 kb, mutations in essential genes, and
258 mutations of genes associated with multi-drug resistance. In addition, once mutations are
259 observed, they are more quickly fixed in the population (Fig. 2k).
260
261 **Construction of a network using WT and essential gene deletion mutants and their**
262 **suppressors**
263
264 To explore the relationships of suppressor mutations from the evolved populations, we
265 established a network of 25 groups, comprising the 24 mutants deleted for essential genes, along
266 with SK36, and their respective evolved suppressors across 249 populations (243 populations
267 from mutants and six populations from SK36). In these 249 populations, 1,272 mutations
268 occurred in 592 distinct segments, with 503 segments belonging to ORFs and 89 belonging to
269 intergenic regions (Fig. 3a, Supplemental Table 4, and Supplemental Table 11-13). This network

270 also encompasses a total of 914 edges connecting these 617 nodes (Fig. 3a and Supplemental
271 Table 11-13).
272
273 Some mutations discovered in the evolved WT also appeared in evolved mutant populations. The
274 twelve mutations occurred in ten distinctive segments, with 5 segments specific to WT and 5
275 shared with populations derived from essential gene mutants. Notably, the ORF J1C87_09360,
276 annotated as PTS mannose/fructose/sorbose transporter family subunit IID, exhibited mutations
277 in two of the six evolved WT populations. This result is consistent with a previous study in
278 SK36, where fitness improvement was associated with mutations in three ORFs of the same
279 operon (J1C87_09355, J1C87_09360, and J1C87_09365).[35] In the current study, mutations in
280 the three OFRs were also observed in mutant populations of Δ*uncH,* Δ*fabG,* Δ*fabK,* Δ*fabF,*
281 Δ*fabZ, and* Δ*pfkA* (Supplementary Fig.6a-b and Supplemental Table 14). Interestingly, most of
282 the evolved populations that contain suppressor mutations in the three PTS
283 mannose/fructose/sorbose transporter subunits are also those that showed the most severe growth
284 defects, such as Δ*fabG,* Δ*fabK,* Δ*fabF,* Δ*fabZ, and* Δ*pfkA* (Fig. 1d and Supplementary Fig.3c).
285 These results demonstrate that mutations in some segments that apparently improved fitness in
286 WT could also contribute to the fitness improvement of essential gene mutants.
287
288 Mutations in some segments that were present in evolved populations deleted of one essential
289 gene also appeared in evolved populations of other mutants deleted of another essential gene. For
290 example, most populations of the mutant deleted for the entire *f1fo* region (*Δf1fo*) and the eight
291 F1Fo subunits deletion mutants (Δ*uncE,* Δ*uncB,* Δ*uncF,* Δ*uncH,* Δ*uncA,* Δ*uncG,* Δ*uncD* and
292 Δ*uncC)* contain suppressor mutations in J1C87_08610 (*trkA1*) and J1C87_08615 (*trkH1*) (Fig.
293 3a). Mutations in many F1Fo subunits are shared among the evolved populations of various other
294 subunit deletion mutants (Fig. 3a and Supplemental Table 4). Furthermore, many of the
295 suppressor mutations in type II fatty acid synthesis (FAS II) gene mutants, such as Δ*fabZ,* Δ*fabF,*
296 Δ*fabG,* Δ*fabK* and Δ*fabH* and those in the CoA biosynthesis mutant Δ*dpcK*, occur in the same
297 ORFs related to fatty acid biosynthesis, including essential genes like acetyl-CoA carboxylase
298 carboxyl transferase subunit alpha (J1C87_09410: *accA*) and acetyl-CoA carboxylase biotin
299 carboxylase subunit (J1C87_09420: *accC*) (Fig. 3a). Similarly, the suppressors identified in the
300 populations of two ribosomal protein mutants *(*Δ*rpmH* and Δ*rplV*) and two GTPase mutants
301 (Δ*yihA* and Δ*obgE*) include mutations in 50S ribosomal protein gene *rplB* (J1C87_00620) and
302 RNA biosynthesis genes, such as *rpoB* (J1C87_01040) (Fig. 3a and Supplemental Table 4).
303 These findings indicate that mutated segments shared across multiple evolved mutants can confer
304 fitness benefits to mutants deleted of different essential genes.
305
306 We also observed mutual suppressors, where an evolved population deleted of the first essential
307 ORF contained a mutated segment within a second essential ORF, while an evolved population
308 deleted of the second essential ORF contained a mutated segment within the first essential ORF.
309 For example, in the *obgE* deletion mutant *(*Δ*obgE*), a mutation in *dnaK* occurred (Fig. 3a and
310 Supplemental Table 4); conversely, in Δ*dnaK*, a mutated segment of *obgE* was detected (Fig. 3a
311 and Supplemental Table 4). Similarly, in the F1Fo subunit deletion mutant Δ*uncF*, a mutation of
312 *dpcK* was also present (Fig. 3a and Supplemental Table 4). In Δ*dpcK*, mutated segments were
313 detected within *uncA* and *uncD* (Fig. 3a and Supplemental Table 4). Other mutual suppressor
314 pairs include those between subunits of F1Fo (Fig. 3a and Supplemental Table 4) and between
315 components of the FASII system (Fig. 3a and Supplemental Table 4). These results suggest the

316 presence of positive epistasis interactions between different essential gene(s), where strains
317 containing mutations in both essential genes are fitter than those containing mutations in either of
318 the essential genes.
319
320 **Possible explanations for parallel suppressor evolution in mutants deleted for particular**
321 **essential genes**
322
323 Given the potential role of parallel evolution for fitness improvement,[36-38] we next sought to
324 identify the most commonly mutated segments for each essential gene mutant and those
325 clustered in a particular operon. Utilizing these highly occurring suppressors (Supplemental
326 Table 4 and Supplemental Table 16), along with candidate genes within duplicated regions (Fig.
327 2b-h), we aimed to elucidate the mechanisms by which they improved the growth of mutants
328 deleted for essential genes.
329
330 Δ*f1fo suppressors*
331 F1Fo is proposed to function as an ATP-dependent proton pump in streptococci, including *S.*
332 *mutans* and *S. sanguinis*.[39] Mutations in *trkA1* or *trkH1* are present in all thirteen evolved
333 populations of Δ*f1fo*, with twelve populations containing *trkH1* mutations and one containing a
334 *trkA1* mutation (Fig. 3b and Supplementary Fig.7, Supplemental Table 4 and Supplemental
335 Table 16). Similarly, mutations in *trkA1*, *trkH1*, or a one base pair (bp) insertion mutation
336 located 38 bp upstream of the *trkA1-H1* operon (P_trkA1-H1, "P" for promoter) are found in
337 twenty-five out of twenty-six (96.2%) of the evolved populations deleted of single F1Fo subunits
338 (Fig. 3b and Supplementary Fig.7, Supplemental Table 4 and Supplemental Table 16). Among
339 the twenty-three mutations in the ORFs of *trkA1-H1*, sixteen populations have *trkH1* mutations,
340 and eight have *trkA1* mutations. Given the comparable length of *trkA1* (1350 bp) and *trkH1*
341 (1440 bp), it appears that mutations in the *trkH1* gene are more likely than mutations in *trkA1* to
342 improve the fitness of mutants deleted for F_1F_o subunits.
343
344 We also observed that gene duplications occurred in the same region across populations deleted
345 of all F1Fo subunits or single subunits, i.e., Δ*f1fo#107* and *#109* (Fig. 2b and Supplementary
346 Fig.4b), Δ*uncE#2* (Supplementary Fig.4c) and Δ*uncH#7* (Fig. 2c). This region of approximately
347 103 kb (coordinates: 22,738-125,834) contains the *v1vo* operon encoding the V1Vo-ATPase,
348 which has been proposed to function as a proton pump[31] and may compensate for the loss of
349 *f1fo*. It is interesting to note that Δ*uncH#7* is the only evolved population listed above that lacks
350 mutations in the flanking upstream regions or the ORFs of *trkA1* or *trkH1* (Fig. 2c). More
351 interestingly, among the evolved populations deleted of F_1F_o subunits (thirteen Δ*f1fo* and twenty-
352 six mutants deleted for single *unc* subunit genes), Δ*uncE#2* and Δ*uncH#7* are the only two
353 populations that contain amino acid substitution mutations of V-type ATP synthase subunits
354 (Supplemental Table 4 and Supplemental Table 16).
355
356 Suppressor mutations appeared in other F1Fo subunits or intergenic regions of *f1fo* in many
357 evolved populations deleted of a single subunit (Fig. 3b and Supplementary Fig.7). This result
358 suggests that for the F_1F_o complex, when one subunit is absent, other subunits cannot function
359 properly and their presence is detrimental to the mutant.
360

361 Given that V1Vo may also function as an ATP-dependent proton pump [31] and the Trk system
362 works as a symporter (K+/Na+ or K+/H+), [40] we hypothesize that *v1vo* can partially compensate
363 for the loss of *f1fo*, that TrkA1-H1 is the major contributor to acidification of the cytosol when
364 pumping in K+, and that the function of TrkA1-H1 must therefore be inhibited when F1Fo is not
365 present (Supplementary Fig.11).
366
367 *ΔftsEX suppressors*
368 FtsEX is crucial in regulating divisome assembly and activation at the plasma membrane and cell
369 wall. [41] In the evolved *ΔftsX* populations, mutations in the *ftsE* gene of the *ftsEX* operon and the
370 *vicRK (vicK/walK* and *vicR/walR)* two-component system (TCS) frequently occurred (Fig. 3b
371 and Supplementary Fig.7). Mutations in *ftsE* were present in eight out of nineteen evolved *ΔftsX*
372 populations (42.1%); in one of these populations, *ΔftsX#13*, a deletion mutation at 51 bp of the
373 693 bp *ftsE* ORF leads to a frameshift in the N-terminal region (Fig. 3b and Supplementary
374 Fig.7). This observation suggests that in the absence of *ftsX*, *ftsE* does not function properly and
375 is deleterious to the cell. Although *vicR* and *vicK* compose a TCS, *vicK* is not essential, while
376 *vicR* is essential. [1,42] Fifteen populations contained *vicK* mutations (with one frameshift and one
377 truncation), and one population contained a *vicR* mutation (an amino acid substitution, M54V),
378 collectively representing 89.5% of the evolved populations (Fig. 3b and Supplementary Fig.7,
379 Supplemental Table 4 and Supplemental Table 16). It was reported that FtsEX interacts with the
380 cell wall component peptidoglycan hydrolase, PcsB, which is positively regulated by the
381 *vicRK/walRK* two-component regulatory system. [43] Therefore, we hypothesize that when FtsEX
382 is absent and PcsB cannot function properly, there is a need to inhibit the activity of PcsB's
383 upstream regulatory factor, VicRK.
384
385 *fab operon suppressors*
386 The *fabH, fabF, fabG, fabZ, and fabK* genes belong to a FASII operon containing thirteen ORFs
387 in total, with a MarR family transcriptional regulator gene (*fabT*) upstream and seven other
388 genes. In the evolved populations of Δ*fabZ,* Δ*fabF,* Δ*fabG,* Δ*fabK,* and Δ*fabH*, we observed a
389 significant enrichment of mutations in genes encoding components of the FASII system (Fig. 3b
390 and Supplementary Fig.7, Supplemental Table 4, and Supplemental Table 16). This result
391 suggests that when one component of the FASII system is deleted, this can trigger genome
392 changes in other FASII components, leading to fitness improvement.
393
394 There is a notable number of populations containing a duplication of approximately 103 kb
395 (coordinate: 22,738-125,834) in the Δ*fabH,* Δ*fabF,* and Δ*fabG* mutants, which includes one ORF
396 encoding an acyltransferase and one ORF encoding acyl carrier protein. Additionally, a
397 duplicated region of 10.1 kb (coordinate: 1,093,824-1,103,958) is shared by Δ*fabZ #1* and Δ*fabZ*
398 *#3* and contains acyl-acyl carrier protein thioesterase. We hypothesize that these duplications
399 may enhance fatty acid synthesis when *fabK, fabZ, fabH, fabF, or fabG* is defective.
400
401 *ΔdpcK suppressors*
402 DPCK is the final enzyme in the five-step pathway for CoA biosynthesis. [44] In the evolved
403 Δ*dpcK* populations*,* mutations ≤100 bp upstream of *acpS* (encoding holo-ACP synthase) are
404 present in eleven of the seventeen Δ*dpcK* populations. Holo-ACP synthase, responsible for
405 covalent attachment of CoA to acyl carrier protein, uses CoA as a substrate for fatty acid
406 biosynthesis. [45] Among the seventeen populations, one population, Δ*dpcK#17,* contained a gene

duplication; we were not able to identify the gene(s) responsible for improved growth due to the large size of the duplication (>300 kb, containing 305 ORFs; Fig. 2i). We hypothesize that holo-ACP synthase is a significant contributor to the use of CoA, and when there is a shortage of CoA, fatty acid production needs to be reduced by lessening the expression of *acpS* (Fig. 3b and Supplementary Fig.7, Supplemental Table 4 and Supplemental Table 15). Consistent with the fitness improvement of Δ*dpcK* by reducing CoA usage, seven out of the seventeen Δ*dpcK* populations contain mutations in the FASII operon (Fig. 3b and Supplementary Fig.7; Supplemental Table 15).

Δ*pfkA suppressors*

pfkA encodes 6-phosphofructokinase (PFK), responsible for catalyzing the phosphorylation of fructose-6-phosphate to fructose-1,6-bisphosphate, a committing step in glycolysis. [46] In the evolved Δ*pfkA* populations, we observed an enrichment of mutations in *fruR, fruB,* and *glck*. Among the ten Δ*pfkA* evolved populations (Fig. 3b and Supplementary Fig.7; Supplemental Table 4, and Supplemental Table 15), six populations contained mutations in *fruR*, five populations had mutations in *fruB*, and nine populations had mutations in *glcK*. The *glcK* gene encodes an ROK domain-containing glucokinase, which phosphorylates glucose to produce glucose-6-phosphate, a progenitor of fructose-6-phosphate. [47] The *fruR* gene encodes a transcriptional repressor of the *fruBA* operon, while *fruB* (also known as *pfkB*) has been demonstrated to function as a 1-phosphofructokinase in multiple bacterial species, [48] including streptococci. [49] Interestingly, the nature of the mutations differed according to the gene; three of the eleven *glcK* mutations were truncations, and four of the seven *fruR* mutations were truncations or frameshift mutations, while none of the seven *fruB* mutations were truncations or frameshifts (Supplemental Table 4 and Supplemental Table 15).

We hypothesize that in the absence of *pfkA*, accumulated fructose-6-phosphate becomes toxic, as has been shown previously in other bacterial species. [48] Elimination of GlcK activity would reduce fructose-6-phosphate production. We further hypothesize that FruB possesses low levels of fructose-6-phosphate kinase activity, thus replacing PfkA, but only when the expression of *fruB* is increased due to *fruR* mutation or the fructose-6-phosphate kinase activity of FruB is increased due to alteration of its sequence. This mechanism would be similar to findings in *E. coli*, where a mutation that increased *fruB* expression was found to suppress the phenotype of Δ*pfkA* mutants. [50,51]

Δ*obgE suppressors*

ObgE belongs to the TRAFAC (Translation Factor Association) class of P-loop GTPases, which is highly conserved and essential in bacteria. [52] The ObgE GTPase is known to play a wide range of functions, with some of the most significant roles including sporulation initiation in *Bacillus subtilis*, [53] aerial mycelium formation in *Streptomyces*, [54,55] bacterial persistence in *E. coli* and *Pseudomonas aeruginosa*, [56] involvement in ribosome biogenesis, [57,58] participation in DNA replication, [59-61] and contributions to chromosome segregation and cell division. [62]

Among the fourteen evolved Δ*obgE* populations, eight populations had substitution mutations upstream of *rpoB* (seven were an A to T mutation 321 bp upstream of the start codon, and the other was an A to G mutation 24 bp upstream), and two populations contained substitution mutations within the *rpoB* ORF (one at 905 bp and the other at 1058 bp from the start of the

453 3567 bp ORF). In total, 71.4% of the populations had mutations within or upstream of *rpoB* (Fig.
454 3b and Supplementary Fig.7;, Supplemental Table 4 and Supplemental Table 15). The *rpoB* gene
455 codes for the beta-subunit of RNA polymerase I. In one of these populations, Δ*obgE#5*, a 37 kb
456 gene duplication was observed (coordinate: 1,775,394-1,812,805), encompassing thirty ORFs,
457 including one annotated as Der GTPase. It was reported that overexpression of *der* or *obgE* can
458 suppress growth defects of a mutant lacking *rrmJ* that encodes the methyltransferase for U2552
459 of the 23S rRNA. [63] From this, we hypothesize that the duplication may partially compensate for
460 the loss of ObgE function by increasing *der* copy numbers, and a reduction in RNA synthesis is a
461 significant fitness adaptation when ObgE is defective.
462
463 <u>*WT and other mutant suppressors*</u>
464 Suppressor mutations in the evolved populations of Δ*pngM*, Δ*yqeG,* Δ*dnaK,* Δ*yihA,* Δ*rpmH,*
465 Δ*rplV,* and WT are less easily explained, and further study is required to identify possible
466 mechanisms (Supplementary Fig.7 and Supplemental Table 15).
467
468 **Testing the working model involving *f1fo, v1vo, trkA1-H1* and *trkA2-H2***
469
470 To test the hypotheses proposed above, we have chosen F1Fo-ATPase, an evolutionarily ancient
471 enzyme complex that is highly conserved across virtually all forms of cellular life [64] and has
472 been reported as essential for entire genus of the streptococcal species. [30]
473
474 We began by testing whether increasing copy numbers of *v1vo* contributes to the fitness
475 improvement of the mutant deleted for the entire F1Fo complex or single subunits. To explore
476 this, we examined the gene duplication of the *v1vo* region at the early stage, P1 in the four
477 populations that contain gene duplications at P6 (Fig. 2b-c, Supplementary Fig.4b-c, and
478 Supplementary Fig.8a). Among these four populations, one had the gene duplication at P1, while
479 the other three acquired the duplication during subsequent passages (Figure 4a and
480 Supplementary Fig.8a). This observation indicates that gene duplications of the *v1vo* region
481 evolved in these populations after initial passages.
482
483 To further confirm the increased fitness of *v1vo* region duplications in populations lacking *f1fo*,
484 we subcultured five *Δf1fo#4* populations from the P6 stage, which did not initially contain gene
485 duplications in the *v1vo* region. After nine additional passages (P15), we observed that two out
486 of the five evolved populations had *v1vo* region duplications in P15 (Fig. 4b and Supplementary
487 Fig.8a).
488
489 To ascertain the fitness improvement by increasing *v1vo* copy numbers in mutants lacking *f1fo*,
490 we tested whether *v1vo* could be deleted in *Δf1fo*. We first deleted the entire *v1vo*, which consists
491 of nine subunits, to generate the *Δv1vo* mutant in the WT background. This *Δv1vo* mutant grew
492 indistinguishably from the wild type in a rich medium (data not shown), demonstrating that *v1vo*
493 can be deleted when *f1fo* is intact (Fig. 4c). However, when we attempted to delete *v1vo* in
494 *Δf1fo#4*, where *f1fo* was removed, it resulted in a double-band genotype in all five *Δv1vo-*
495 *DB/Δf1fo#4* ("DB" for double-band) lines tested (Fig. 4c and Supplementary Fig.9). Consistent
496 with these findings, Δ*uncE#2* and Δ*uncH#7*, which contain amino acid substitution mutations of
497 V1Vo ATP synthase subunit A and K in the *v1vo* operon, respectively, also contain *v1vo* region
498 duplications (Supplemental Table 4). This finding indicates that increased copy numbers of the

499 *v1vo* genes compensated for the loss of F1Fo function. Overall, these results suggest that
500 increasing the copy numbers of *v1vo* contributes to the fitness improvement of mutants lacking
501 *f1fo*.
502
503 We then investigated the impact of inhibiting *trkA1-H1* on enhancing the fitness of *Δf1fo*.
504 Initially, we compared the occurrence of *trkA1-H1* mutations between P1 and P6 stages across
505 twelve independently evolved populations of *Δf1fo* (*#101* to *#112*). While mutations in the *trkA1*
506 or *trkH1* segments were not detected in P1 using a 30% threshold in nine of the twelve
507 populations, we observed *trkA1-H1* mutations in all populations, with the mutation frequency
508 increasing during passage in all six independently evolved populations (Fig. 4d and Table S17).
509 These mutations resulted in at least one frameshift and various substitutions in the translation of
510 TrkA1 or TrkH1 in six populations, while in the remaining populations, they led to a histidine
511 insertion or various substitutions in the TrkH1 protein (Supplemental Table 16). This data
512 indicates the fixation of *trkA1-H1* mutations during passage.
513
514 To further investigate the impact of *trkA1-H1*, we compared the growth of *Δf1fo* in the presence
515 and absence of *trkA1-H1*. *S. sanguinis* SK36 has two Trk systems, *trkA1-H1* and *trkA2-H2*. The
516 growth of *trkH2*, or double-gene deletion mutants of *trkA1-H1* or *trkA2-H2,* were
517 indistinguishable from that of WT (Fig. 4e, Supplementary Fig.10a-f and Supplemental Table
518 17). However, combined deletion of either *trkA1* or *trkH1* along with *trkH2* resulted in growth
519 defects (Fig. 5e-g, Supplementary Fig.10g-h, and Supplemental Table 17), indicating that *trkA1-*
520 *H1* and *trkA2-H2* are redundant for growth. In order to determine the effect of mutating the two
521 Trk systems on the fitness of *Δf1fo*, we transformed the *Δf1fo* construct into the backgrounds of
522 *ΔtrkA1-H1*or *ΔtrkA2-H2*, and compared the growth of the *Δf1fo/ ΔtrkA1-H1* mutant and that of
523 *Δf1fo/ΔtrkA2-H2*. As controls, we also included *Δf1fo#4*, which contains a frameshift mutation of
524 *ΔtrkH1* in the *Δf1fo* background (Supplemental Table 4). It showed that while the growth of
525 *Δf1fo#4* and *Δf1fo/ΔtrkA1-H1* were comparable to each other, the growth of *Δf1fo/ΔtrkA2-H2*
526 was significantly inhibited compared to that of *Δf1fo#4* and *Δf1fo/ΔtrkA1-H1.* (Fig. 4f-g and
527 Supplemental Table18). These findings suggest that inhibiting *trkA1-H1*, but not *trkA2-H2*,
528 contributes to the fitness improvement of evolved mutants deleted for *f1fo*.
529
530 In lactic acid bacteria, F1Fo-ATPase is believed to function by pumping out protons to alkalinize
531 the cytosol or to build negative internal and positive external membrane potentials. [65] To test
532 whether the growth defects in the *S. sanguinis Δf1fo* mutant are due to impaired function in
533 alkalinizing the cytosol or building a membrane potential, we compared the growth of *Δf1fo#4* in
534 a rich medium supplemented with lactic acid (which increases membrane potential and cytosolic
535 proton concentration) or NaOH (which lowers membrane potential and cytosolic proton
536 concentration). We observed that *Δf1fo#4* is susceptible to lactic acid treatment compared to WT
537 (Fig. 4h and Supplemental Table 18). Conversely, the growth defect of *Δf1fo#4* can be partially
538 rescued by NaOH within a certain range (Fig. 4i and Supplemental Table 18). These results
539 suggest that *f1fo* in *S. sanguinis* functions by pumping out protons to alkalinize the cytosol.
540
541 We therefore suggest the following model for the relationship of *f1fo* with *v1vo, trkA1-H1,* and
542 *trkA2-H2* (Supplementary Fig.11). For streptococci, which do not contain the tricarboxylic acid
543 cycle or electron transport chain, energy production is mainly through lactic acid fermentation. [66]
544 The lactate from fermentation creates highly acidic cytosol, which would be toxic if H+ were not

exported. F1Fo pumps out H+ from the cytosol using ATP. Both TrkA1-H1 and TrkA2-H2 are potassium transporters and functionally redundant for that purpose. TrkA1-H1 pumps in potassium together with H+, acidifying the cytosol when H+ is not exported. In contrast, TrkA2-H2 does not pump protons into the cytosol when pumping in potassium (likely instead pumping in Na+). Therefore, the function of TrkA1-H1 must be inhibited if F1Fo is not functional.

Conserved functional relationships of *f1fo*, *trkA1-H1*, *trkA2-H2* and *v1vo* in different streptococci

To generalize the *f1fo* working model and assess F1Fo's essentiality in other strains and species, we conducted essentiality evaluations in three other streptococci: *S. mutans* UA159, *S. sanguinis* SK405, and *S. sanguinis* SK1058. Genomic sequencing of *S. mutans* UA159, [67] *S. sanguinis* SK405 [33,] and *S. sanguinis* SK1058 [33] showed that *f1fo* and *trkA1-H1* are present in all three strains, as in SK36, while *v1vo* is present in the *S. sanguinis* strains only. *TrkA2-H2* is present in both *S. sanguinis* SK36 and SK405 but not in *S. sanguinis* SK1058 or *S. mutans* UA159 (Fig. 5a).

To assess whether *v1vo* could serve as a partial backup in cases of F1Fo loss-of-function, we attempted to delete *f1fo* in *S. mutans* UA159, which lacks *v1vo*. Despite multiple attempts and a total of 64 independent genotyping analyses, none of the transformants were deleted for *f1fo*, instead producing a double band indicative of gene duplication prior to allelic exchange (Supplementary Fig.12a-b). This result highlights that in *S. mutans* UA159, lacking *v1vo, f1fo* cannot be deleted in our conditions. This observation supports the evolutionarily conserved relationship between *f1fo* and *v1vo* observed in other streptococcal species.

We then investigated the impact of deleting *trkA1-H1* in the other two strains: *S. sanguinis* SK1058, which only possesses *trkA1-H1*, and *S. sanguinis* SK405, which has both *trkA1-H1* and *trkA2-H2*. Our findings showed that *trkA1-H1* mutants exhibited severe growth defects in the SK1058 background compared to the SK405 background (Supplementary Fig.13a-c). This result demonstrates the requirements of the *Trk* system for growth within the species of *S. sanguinis*.

Next, we investigated the possibility of deleting *f1fo* in *S. sanguinis* SK1058 and SK405, both of which contain *v1vo* and *trkA1-H1*. We could generate *f1fo* whole-region deletion mutants (*Δf1fo*) in both SK1058 and SK405 backgrounds (Fig. 5b, 5c, Supplementary Fig.14). Furthermore, the growth of mutants with *f1fo* deletions in SK405 was notably better than in SK1058 (Fig. 5b, 5d, and Supplemental Table 19). To explore the potential emergence of *trkA1-H1* suppressor mutations during evolution, we conducted passage experiments using independently evolved populations with *f1fo* deletions in SK405 (Supplementary Fig.14a: three populations) and in SK1058 (Supplementary Fig.14b: two populations). It was observed that, after six passages, *trkA1-H1* suppressor mutations appeared in all evolved *Δf1fo* populations in SK405 and SK1058 (Fig. 5e). At least one population each in the SK405 and SK1058 backgrounds are frameshift or truncation mutations of *trkA1-H1* (Fig. 7e and Supplemental Table 20). This result underscores the evolutionarily conserved occurrence of *trkA1-H1* suppressor mutations in evolved populations with *f1fo* deletions.

Discussion

591
592 While identifying genes that interact with essential genes or compensate for their loss provides a
593 great benefit, [4] this task remains challenging, primarily due to the unavailability of essential-gene
594 deletion mutants and systematic methodologies to connect the function of essential genes with
595 their partners. Traditional approaches, such as antisense RNA knockdowns [48] and CRISPR
596 interference, [68,69] while valuable, may exhibit limitations, including incomplete target gene
597 silencing and suboptimal design efficacy, [69] thereby potentially compromising the reliability of
598 essential gene functional analyses. Our study successfully established a system to generate viable
599 mutants with deletions in essential genes (Fig. 1 and Supplementary Fig.1-S2). We observed that
600 small colonies likely represent the deletion mutants, while large colonies often exhibit the
601 "double-band" genotype or kanamycin resistance due to mutations in translational machinery.
602
603 With these observations, we have generated essential gene deletion mutants, many of which are
604 also essential across multiple species (http://www.essentialgene.org/). These essential gene
605 mutants provide an invaluable resource for dissecting the functions of essential genes. Using
606 these twenty-four essential gene mutants and WT as controls, we identified over 1000
607 spontaneous suppressor mutations in passage experiments (Fig. 2). Leveraging these essential
608 gene mutants and distinct mutated segments, we constructed a functional network (Fig. 3a).
609 Within this network, we made several noteworthy observations. 1) Mutated segments that
610 appeared in the evolved WT population can also appear in the evolved populations of mutants
611 with deletions of essential genes, such as mutations in the PTS mannose/fructose/sorbose
612 transporter family subunit. 2) Suppressor mutations in certain genes, such as *rpoB* and *rpsL,* that
613 are found in the evolved populations of one deletion mutant can also be present in the evolved
614 populations of other mutants (Supplemental Table 4). 3) Mutual essential gene suppressor
615 mutations were discovered, where mutations in the first essential gene were found within a
616 mutant population deleted for the second essential gene, and vice versa.
617
618 As expected, our findings support the notion that mutants with deletions of essential genes face
619 stronger selective pressures when compared to that of the WT. These mutants are more likely to
620 undergo the following significant evolutionary changes. 1) Gene duplications of greater than 10
621 kb: Our data revealed large-scale gene duplications exclusively were present in mutants deleted
622 of essential genes (Fig. 2b-h). 2) Substitutions, insertions, and deletions of less than 10 kb:
623 Small-scale mutations, especially those of >50% of sequence reads, were more common in
624 mutants deleted for essential genes (Fig. 2i). 3) Mutations in essential genes: Mutations in other
625 essential genes were observed more exclusively in mutants deleted for an essential gene (Fig.
626 2k). 4) Mutations in multi-drug resistance genes: mutations of multi-drug resistance-associated
627 genes, such as *rpoB* and *rpsL,* are present in several evolved populations deleted for essential
628 genes, suggesting a shared selective pressure resulting from drug treatment and deletion of
629 essential genes (Supplemental Table 4). The suppressor mutations identified in our evolved
630 populations deleted of essential genes may reflect the differential gene essentiality over
631 evolutionary time in the pan-genome [11] and reproducibly changing gene essentiality across
632 independently evolving populations. [13]
633
634 Unexpectedly, as discussed above, for every essential gene mutated, we identified at least one
635 population containing a suppressor mutation in another essential gene (Fig. 2l). Notably, the
636 essential genes were inactivated by the suppressor mutation in some of the evolved populations,

637 such as the >200bp insertion mutation in *ftsZ* in the evolved population of *Δf1fo #107*, the >200
638 bp deletion mutation of *uncH* in *ΔuncC#1*, and the 1 bp deletion mutation of *ftsE* in *ΔftsX#13*
639 (Supplemental Table 4). In contrast, for other essential gene mutation suppressors, the mutations
640 were not within the open reading frame (ORF) but were found within 400 base pairs upstream of
641 the start codons, likely affecting expression rather than inactivating function. For instance, in the
642 evolved *ΔdpcK* populations, the suppressors with the highest mutation frequency were located
643 upstream of the holo-ACP synthase gene, *acpS* (Supplementary Fig.5). Similarly, in the evolved
644 *ΔobgE* populations, the majority of mutation suppressors were found upstream of *rpoB*
645 (Supplementary Fig.5).
646
647 Essential genes represent ideal drug targets for controlling infectious diseases and cancers. In
648 traditional medical treatment, the focus has primarily been on targeting a single essential gene
649 product. However, it's crucial to consider the evolution of gene essentiality during drug treatment
650 and the development of drug resistance over short-term evolution. We have observed that in
651 multiple populations deleted of essential genes, mutations in multiple segments appeared within
652 six passages, including those belonging to multi-drug resistance-associated genes (Fig. 2m).
653 Considering that some of the suppressor mutations were gene duplications that presumably
654 confer fitness benefits by increasing gene copy numbers, a promising approach is to target not
655 only the essential gene itself but also the backup gene. This strategy can help prevent or reduce
656 the development of drug resistance.
657
658 To understand the relationships between the structure and function of a protein, it is of great
659 interest to know which amino acids or domains of the proteins are sensitive to mutations. In this
660 study, we have observed numerous mutations of *trkA1* and *trkH1* in *Δf1fo* or *f1fo* single subunit
661 deletion mutants, *vicK* in *ΔftsX*, *fruR* and *glcK* in *ΔpfkA*, as well as *fusA*, *rpsL* and *rplF* in
662 kanamycin-resistant mutants lacking the *kan* gene (Supplemental Table 1-2). These mutations
663 represent fitness-related protein sequence changes that improve the growth of resultant mutants
664 in a particular selective condition.
665
666 In this work, we have demonstrated the efficacy of the methodology developed for generating
667 deletion mutants of numerous essential genes in *S. sanguinis* SK36. Furthermore, we have
668 highlighted the potency of experimental evolution [24,25] in unraveling the mechanisms of gene
669 essentiality, with a particular focus on *f1fo* in *S. sanguinis* and *S. mutans*. It would be interesting
670 to test the conservation or divergence of mechanisms governing gene essentiality of other genes,
671 as well as across different *Streptococcus* species and other genera. While extracting valuable
672 information by identifying spontaneous suppressor mutations in populations lacking essential
673 genes is possible, conducting experimental evolution requires caution. First and foremost, the
674 choice of an appropriate organism is crucial. Ideally, the selected organism should have a single
675 chromosome, a small genome size, and a rapid cell division rate. Streptococci represent an ideal
676 candidate in this regard. They possess a single circular genome with a relatively modest size,
677 typically ranging from 2.0 to 3.0 megabases. [70] This choice contrasts with a previous study that
678 employed budding yeast with multiple chromosomes [4] where most mutations in populations
679 lacking essential genes were related to changes in ploidy, which could hinder the identification
680 of causal suppressors. On the other hand, the identification of mechanisms of genetic suppression
681 requires caution. For the suppressor mutations of low frequency or these substitution mutations
682 where we were unable to determine whether the evolved suppressor mutations increase or

683 decrease the activity of the gene product, further evidence is needed to understand the
684 mechanisms underlying the evolution of gene essentiality.
685
686 In general, essential genes tend to be more conserved and evolutionarily ancient compared to
687 non-essential genes. [54] It is intriguing to consider when genes emerge within a biological system
688 over time. The suppressor mutations in essential gene mutants, particularly the loss-of-function
689 mutations, can provide valuable insights into dependency relationships. For instance, the absence
690 of *f1fo* in a system may hinder the emergence of the *trkA1-H1* system. In cases where essential
691 genes function as a complex, such as *f1fo* or *ftsEX*, our findings indicate that deletion of one
692 component may result in additional deleterious effects caused by the remaining subunit(s)
693 (Supplemental Table 4). This suggests that all subunits of the complex need to be integrated into
694 the system, at least for these cases. Moreover, understanding the timelines of gene emergence in
695 a system is also crucial for guiding decisions in synthetic biology, determining which genes, as
696 well as the order of genes, to be introduced into a system.
697
698 **Materials and Methods**
699
700 *Strains Used and Growth Conditions:*
701 In this study, we primarily utilized *Streptococcus sanguinis* strain SK36. [27] *S. sanguinis* SK405
702 and SK1058 strains were described previously. [33] *S. mutans* UA159 was obtained from Ann
703 Progulske-Fox (University of Florida). All bacterial cultures were routinely maintained in a BHI
704 medium at 37°C under anaerobic conditions, using a Coy anaerobic chamber, or stored at -80 °C
705 for long-term storage.
706
707 *Transformation and Mutant Isolation:*
708 To prepare competent cells, *S. sanguinis* was cultured in 1 mL of Todd-Hewitt + HS medium [10]
709 and incubated overnight in anaerobic conditions at 37°C. The following day, a 5 µL aliquot of
710 the overnight culture was added to 1 mL of fresh TS+HS medium and incubated for an additional
711 3 hours.
712
713 For creating knockout constructs, we employed 1 kb of homologous 3' and 5' end sequences
714 flanking the coding sequence (CDS) and resistance genes, *kan* or *Erm*^{r}, in overlapping extension
715 PCR (for primers used, see Supplemental Table 21). [27] For transformation, we mixed 50 ng to
716 500 ng of PCR product DNA with 200 ng of CSP and 300 µL of competent cells. The reactions
717 continued for 24 hours under anaerobic conditions at 37°C. Subsequently, transformation
718 reaction mixtures were plated on BHI-agar containing appropriate antibiotics (Kanamycin: 500
719 µg/mL or Erythromycin: 10 µg/mL) for selection. Once the plates had dried, the cells were
720 overlaid with a thin layer of agar by adding 1 mL of cooled BHI-agar with antibiotics. The plates
721 were incubated at 37°C under anaerobic conditions to select transformants for 4 to 5 days.
722
723 For genotyping, genomic DNA (gDNA) was isolated from 2 mL of saturated cultures. In brief,
724 cells were precipitated by centrifugation at 10,000 rpm for 10 minutes at room temperature. They
725 were then resuspended in 200 µL of resuspension buffer (20 mM EDTA, 200 mM Tris-HCl, and
726 2% Triton-X 100) and lysed with 200 µL of AL lysis buffer (Qiagen, 19075). DNA was
727 precipitated by adding 1 mL of 100% ethanol supplemented with 100 mM of sodium acetate.

728 Following washing and drying, the DNA was dissolved in 100 µL of water and used for PCR
729 and/or whole-genome sequencing.
730
731 To generate deletion mutants *Δf1fo* in *ΔtrkA1-H1* and *ΔtrkA2-H2*, the *ΔtrkA1-H1* and *ΔtrkA2-H2*
732 mutants were first generated using *Erm*^{r} (Supplementary Fig.10). After confirmation of deletion
733 of *ΔtrkA1-H1* and *ΔtrkA2-H2, Δf1fo* of *kan* resistance construct was subsequentially transformed
734 into *ΔtrkA1-H1* or *ΔtrkA2-H2.* To generate deletion mutants of both *trkA1-H1* and *trkA2-H2*,
735 *trkA1, trkH1*, or *ΔtrkA1-H1* of erythromycin resistance constructs were transformed into a
736 *ΔtrkH2* mutant of kan resistance background (Xu, et al., 2011). To isolate *Δf1fo* and *ΔtrkA1-H1*
737 mutants in the SK405 and SK1058 strains, we employed the same PCR construct used for
738 deleting *f1fo* and *trkA1-H1* in SK36, as there is >90% identity at the flanking regions between
739 SK36, SK1058, and SK405.
740
741 *Strain Passage:*
742 Antibiotic-resistant colonies from selection plates were transferred to 1 mL of BHI containing
743 antibiotics and grown for 2 to 8 days under anaerobic conditions at 37°C. The duration depended
744 on when the OD_{600} reached 0.1-0.5, which was referred to as P0. A 300 µL aliquot of the cell
745 culture was then transferred to 3 mL of BHI containing antibiotics, and growth continued until
746 saturation, resulting in P1. P1 was mixed by pipetting five times with a P-1000 pipette, and 50
747 µL of the mixed P1 was transferred to 1 mL of BHI containing antibiotics. Growth proceeded
748 until the cell culture reached an OD_{600} of 0.1 to 0.5, producing P2. The latter process was
749 repeated sequentially from P3 to P6, where the volume of P2 to P5 was 1 mL and the final
750 passage, P6 was 3 mL. Cell cultures of P1 and P6 were stored at -80°C in glycerol at the final
751 concentration of 20%. DNA extractions and genome sequencing were conducted in P6 and/or P1
752 when indicated.
753
754 For passages involving WT, glycerol stocks from -80°C were transferred to 1 mL of BHI and
755 grown for 24 hours, resulting in T0 (see Supplementary Fig.4a). A 50 µL aliquot of T0 cell
756 culture was aliquoted into six 1.5 mL tubes, each containing 1 mL of BHI, and grown for 24
757 hours, resulting in T1. A 50 µL aliquot of T1 cell culture was inoculated into 1 mL of BHI and
758 grown for 24 hours, leading to T2. This process was repeated for T3 to T9.
759
760 *Whole-Genome Sequencing and Variant Calling:*
761 Whole-genome sequencing was carried out by the Genome Core at Virginia Commonwealth
762 University or by SeqCenter (https://www.seqcenter.com/) using the shotgun method with 2x150
763 paired-end sequencing. Whole-genome sequences with an average coverage of ≥200 were used
764 for subsequent analysis.
765
766 Fastq files were aligned to the SK36 reference genome [16] using Geneious Prime software
767 (https://www.geneious.com/) after trimming via the BBDuk method. Variations in the genome
768 were exported from Geneious Prime. To identify the mutated segment, the frequencies
769 (percentages) of all mutations belonging to a certain segment were assessed and the greatest
770 value of percentages were assigned to that segment. For the deletions, the read coverages were
771 calculated by averaging the base coverages that were 100 bp from the flanking sequence. For
772 network analysis, the software Cytoscape was used.[71]
773

Data and materials availability

All data needed to evaluate the conclusions in the paper are present in the paper and/or the Supplementary files. The genome sequence data will be deposited to BioProject (PRJNA1146876). All the transgenic materials, including the essential gene deletion mutants are available from the authors upon request.

Contributions

L.B. and P.X. conceived the project. L.B., T.K. and P.X. designed the experiments. L.B. constructed all the essential gene mutants and performed all experimental evolution studies. L.B., T.K., and P.X. analyzed the data with the help of Z.Z., A.I., B.Z., V.A. and M.W. The manuscript was written and revised by L.B., T.K., and P.X.

Acknowledgments

The authors would like to thank Dr. Mark Running at the Department of Biology, University of Louisville, Dr. Tomomichi Fujita at the Department of Biological Sciences, Hokkaido University, Dr. Tim van Opijnen at Broad Institute, MIT and Harvard, and Dr. Yan Bao at the School of Agriculture and Biology, Shanghai Jiao Tong University, for discussions regarding experimental design and critical reading of the manuscript. We also thank Dr. Junling Ren at the Philips Institute for Oral Health Research, Virginia Commonwealth University for help with network analysis and Ms. Ayana Wyche at Virginia Commonwealth University for assistance with the culturing of bacteria. We are grateful to Vladimir Lee and Kalyan Maliempati for genomic sequencing services. This work was funded by grants from the National Institutes of Health R01DE030121 (P.X. and T.K.) and the CCTR Endowment Fund (P.X.).

Declaration of generative AI in scientific writing

During the preparation of this work the authors used ChatGPT-3 in order to improve readability and language. After using it, the authors reviewed and edited the content as needed and took full responsibility for the content of the publication.

Declaration of interests

A patent application has been submitted by P.X. and L.B. and the Virginia Commonwealth University based on these results.

References

1. Xu, P., Ge, X., Chen, L., Wang, X., Dou, Y., Xu, J.Z., Patel, J.R., Stone, V., Trinh, M., Evans, K., et al. (2011). Genome-wide essential gene identification in *Streptococcus sanguinis*. Scientific reports *1*, 125. 10.1038/srep00125.
2. Rancati, G., Moffat, J., Typas, A., and Pavelka, N. (2018). Emerging and evolving concepts in gene essentiality. Nat Rev Genet *19*, 34-49. 10.1038/nrg.2017.74.

3. Costanzo, M., VanderSluis, B., Koch, E.N., Baryshnikova, A., Pons, C., Tan, G., Wang, W., Usaj, M., Hanchard, J., Lee, S.D., et al. (2016). A global genetic interaction network maps a wiring diagram of cellular function. Science *353*. 10.1126/science.aaf1420.
4. Jana, B., Liu, X., Dénéréaz, J., Park, H., Leshchiner, D., Liu, B., Gallay, C., Veening, J.W., and van Opijnen, T. (2023). CRISPRi-TnSeq: A genome-wide high-throughput tool for bacterial essential-nonessential genetic interaction mapping. bioRxiv. 10.1101/2023.05.31.543074.
5. Nijman, S.M. (2011). Synthetic lethality: general principles, utility and detection using genetic screens in human cells. FEBS Lett *585*, 1-6. 10.1016/j.febslet.2010.11.024.
6. Leaver, M., Domínguez-Cuevas, P., Coxhead, J.M., Daniel, R.A., and Errington, J. (2009). Life without a wall or division machine in *Bacillus subtilis*. Nature *457*, 849-853. 10.1038/nature07742.
7. Mutschler, H., Gebhardt, M., Shoeman, R.L., and Meinhart, A. (2011). A novel mechanism of programmed cell death in bacteria by toxin-antitoxin systems corrupts peptidoglycan synthesis. PLoS Biol *9*, e1001033. 10.1371/journal.pbio.1001033.
8. Larrimore, K.E., and Rancati, G. (2019). The conditional nature of gene essentiality in *Pseudomonas aeruginosa*. Curr Opin Genet Dev *58-59*, 55-61. 10.1016/j.gde.2019.07.015.
9. Liu, G., Yong, M.Y., Yurieva, M., Srinivasan, K.G., Liu, J., Lim, J.S., Poidinger, M., Wright, G.D., Zolezzi, F., Choi, H., et al. (2015). Gene Essentiality Is a Quantitative Property Linked to Cellular Evolvability. Cell *163*, 1388-1399. 10.1016/j.cell.2015.10.069.
10. Rancati, G., Pavelka, N., Fleharty, B., Noll, A., Trimble, R., Walton, K., Perera, A., Staehling-Hampton, K., Seidel, C.W., and Li, R. (2008). Aneuploidy underlies rapid adaptive evolution of yeast cells deprived of a conserved cytokinesis motor. Cell *135*, 879-893. 10.1016/j.cell.2008.09.039.
11. Bao, L., Inoue, N., Ishikawa, M., Gotoh, E., Teh, O.K., Higa, T., Morimoto, T., Ginanjar, E.F., Harashima, H., Noda, N., et al. (2022). A PSTAIRE-type cyclin-dependent kinase controls light responses in land plants. Sci Adv *8*, eabk2116. 10.1126/sciadv.abk2116.
12. Rosconi, F., Rudmann, E., Li, J., Surujon, D., Anthony, J., Frank, M., Jones, D.S., Rock, C., Rosch, J.W., Johnston, C.D., and van Opijnen, T. (2022). A bacterial pan-genome makes gene essentiality strain-dependent and evolvable. Nat Microbiol *7*, 1580-1592. 10.1038/s41564-022-01208-7.
13. Couce, A., Limdi, A., Magnan, M., Owen, S.V., Herren, C.M., Lenski, R.E., Tenaillon, O., and Baym, M. (2024). Changing fitness effects of mutations through long-term bacterial evolution. Science *383*, eadd1417. 10.1126/science.add1417.
14. Santamaría, D., Barrière, C., Cerqueira, A., Hunt, S., Tardy, C., Newton, K., Cáceres, J.F., Dubus, P., Malumbres, M., and Barbacid, M. (2007). Cdk1 is sufficient to drive the mammalian cell cycle. Nature *448*, 811-815. 10.1038/nature06046.
15. Nowack, M.K., Harashima, H., Dissmeyer, N., Zhao, X.A., Bouyer, D., Weimer, A.K., De Winter, F., Yang, F., and Schnittger, A. (2012). Genetic framework of cyclin-dependent kinase function in *Arabidopsis*. Dev. Cell *22*, 1030-1040. 10.1016/j.devcel.2012.02.015.
16. Glass, J.I., Merryman, C., Wise, K.S., Hutchison, C.A., and Smith, H.O. (2017). Minimal Cells-Real and Imagined. Cold Spring Harb Perspect Biol *9*. 10.1101/cshperspect.a023861.

866 17. Juhas, M., Eberl, L., and Church, G.M. (2012). Essential genes as antimicrobial targets
867 and cornerstones of synthetic biology. Trends Biotechnol *30*, 601-607.
868 10.1016/j.tibtech.2012.08.002.
869 18. Hutchison, C.A., Chuang, R.Y., Noskov, V.N., Assad-Garcia, N., Deerinck, T.J.,
870 Ellisman, M.H., Gill, J., Kannan, K., Karas, B.J., Ma, L., et al. (2016). Design and
871 synthesis of a minimal bacterial genome. Science *351*, aad6253.
872 10.1126/science.aad6253.
873 19. Ratcliff, W.C., Denison, R.F., Borrello, M., and Travisano, M. (2012). Experimental
874 evolution of multicellularity. Proc Natl Acad Sci U S A *109*, 1595-1600.
875 10.1073/pnas.1115323109.
876 20. Blount, Z.D., Borland, C.Z., and Lenski, R.E. (2008). Historical contingency and the
877 evolution of a key innovation in an experimental population of *Escherichia coli*. Proc
878 Natl Acad Sci U S A *105*, 7899-7906. 10.1073/pnas.0803151105.
879 21. Moger-Reischer, R.Z., Glass, J.I., Wise, K.S., Sun, L., Bittencourt, D.M.C., Lehmkuhl,
880 B.K., Schoolmaster, D.R., Lynch, M., and Lennon, J.T. (2023). Evolution of a minimal
881 cell. Nature *620*, 122-127. 10.1038/s41586-023-06288-x.
882 22. Kawecki, T.J., Lenski, R.E., Ebert, D., Hollis, B., Olivieri, I., and Whitlock, M.C. (2012).
883 Experimental evolution. Trends Ecol Evol *27*, 547-560. 10.1016/j.tree.2012.06.001.
884 23. Barrick, J.E., and Lenski, R.E. (2013). Genome dynamics during experimental evolution.
885 Nat Rev Genet *14*, 827-839. 10.1038/nrg3564.
886 24. McDonald, M.J. (2019). Microbial Experimental Evolution - a proving ground for
887 evolutionary theory and a tool for discovery. EMBO Rep *20*, e46992.
888 10.15252/embr.201846992.
889 25. Van den Bergh, B., Swings, T., Fauvart, M., and Michiels, J. (2018). Experimental
890 Design, Population Dynamics, and Diversity in Microbial Experimental Evolution.
891 Microbiol Mol Biol Rev *82*. 10.1128/MMBR.00008-18.
892 26. Taylor, T.B., Mulley, G., Dills, A.H., Alsohim, A.S., McGuffin, L.J., Studholme, D.J.,
893 Silby, M.W., Brockhurst, M.A., Johnson, L.J., and Jackson, R.W. (2015). Evolutionary
894 resurrection of flagellar motility via rewiring of the nitrogen regulation system. Science
895 *347*, 1014-1017. 10.1126/science.1259145.
896 27. Xu, P., Alves, J.M., Kitten, T., Brown, A., Chen, Z., Ozaki, L.S., Manque, P., Ge, X.,
897 Serrano, M.G., Puiu, D., et al. (2007). Genome of the opportunistic pathogen
898 *Streptococcus sanguinis*. J Bacteriol *189*, 3166-3175. 10.1128/JB.01808-06.
899 28. Lázár, V., Pal Singh, G., Spohn, R., Nagy, I., Horváth, B., Hrtyan, M., Busa-Fekete, R.,
900 Bogos, B., Méhi, O., Csörgő, B., et al. (2013). Bacterial evolution of antibiotic
901 hypersensitivity. Mol Syst Biol *9*, 700. 10.1038/msb.2013.57.
902 29. Rhodes, D.V., Crump, K.E., Makhlynets, O., Snyder, M., Ge, X., Xu, P., Stubbe, J., and
903 Kitten, T. (2014). Genetic characterization and role in virulence of the ribonucleotide
904 reductases of *Streptococcus sanguinis*. J Biol Chem *289*, 6273-6287.
905 10.1074/jbc.M113.533620.
906 30. Luo, H., Lin, Y., Gao, F., Zhang, C.T., and Zhang, R. (2014). DEG 10, an update of the
907 database of essential genes that includes both protein-coding genes and noncoding
908 genomic elements. Nucleic Acids Res *42*, D574-580. 10.1093/nar/gkt1131.
909 31. Nelson, N., Perzov, N., Cohen, A., Hagai, K., Padler, V., and Nelson, H. (2000). The
910 cellular biology of proton-motive force generation by V-ATPases. J Exp Biol *203*, 89-95.
911 10.1242/jeb.203.1.89.

912 32. Röttig, A., and Steinbüchel, A. (2013). Acyltransferases in bacteria. Microbiol Mol Biol
913 Rev *77*, 277-321. 10.1128/MMBR.00010-13.
914 33. Baker, S.P., Nulton, T.J., and Kitten, T. (2019). Genomic, Phenotypic, and Virulence
915 Analysis of *Streptococcus sanguinis* Oral and Infective-Endocarditis Isolates. Infect
916 Immun *87*. 10.1128/IAI.00703-18.
917 34. Ghosh, A., N, S., and Saha, S. (2020). Survey of drug resistance associated gene
918 mutations in Mycobacterium tuberculosis, ESKAPE and other bacterial species.
919 Scientific reports *10*, 8957. 10.1038/s41598-020-65766-8.
920 35. Zeng, L., Walker, A.R., Lee, K., Taylor, Z.A., and Burne, R.A. (2021). Spontaneous
921 Mutants of Streptococcus sanguinis with Defects in the Glucose-Phosphotransferase
922 System Show Enhanced Post-Exponential-Phase Fitness. J Bacteriol *203*, e0037521.
923 10.1128/JB.00375-21.
924 36. Chevin, L.M., Martin, G., and Lenormand, T. (2010). Fisher's model and the genomics of
925 adaptation: restricted pleiotropy, heterogenous mutation, and parallel evolution.
926 Evolution *64*, 3213-3231. 10.1111/j.1558-5646.2010.01058.x.
927 37. Wichman, H.A., Badgett, M.R., Scott, L.A., Boulianne, C.M., and Bull, J.J. (1999).
928 Different trajectories of parallel evolution during viral adaptation. Science *285*, 422-424.
929 10.1126/science.285.5426.422.
930 38. Stern, D.L. (2013). The genetic causes of convergent evolution. Nat Rev Genet *14*, 751-
931 764. 10.1038/nrg3483.
932 39. Sheng, J., and Marquis, R.E. (2006). Enhanced acid resistance of oral streptococci at
933 lethal pH values associated with acid-tolerant catabolism and with ATP synthase activity.
934 FEMS Microbiol Lett *262*, 93-98. 10.1111/j.1574-6968.2006.00374.x.
935 40. Corratgé-Faillie, C., Jabnoune, M., Zimmermann, S., Véry, A.A., Fizames, C., and
936 Sentenac, H. (2010). Potassium and sodium transport in non-animal cells: the
937 Trk/Ktr/HKT transporter family. Cell Mol Life Sci *67*, 2511-2532. 10.1007/s00018-010-
938 0317-7.
939 41. Du, S., Pichoff, S., and Lutkenhaus, J. (2016). FtsEX acts on FtsA to regulate divisome
940 assembly and activity. Proc Natl Acad Sci U S A *113*, E5052-5061.
941 10.1073/pnas.1606656113.
942 42. Moraes, J.J., Stipp, R.N., Harth-Chu, E.N., Camargo, T.M., Höfling, J.F., and Mattos-
943 Graner, R.O. (2014). Two-component system VicRK regulates functions associated with
944 establishment of *Streptococcus sanguinis* in biofilms. Infect Immun *82*, 4941-4951.
945 10.1128/IAI.01850-14.
946 43. Sham, L.T., Barendt, S.M., Kopecky, K.E., and Winkler, M.E. (2011). Essential PcsB
947 putative peptidoglycan hydrolase interacts with the essential FtsXSpn cell division
948 protein in *Streptococcus pneumoniae* D39. Proc Natl Acad Sci U S A *108*, E1061-1069.
949 10.1073/pnas.1108323108.
950 44. Gupta, A., Singh, P.K., Sharma, P., Kaur, P., Sharma, S., and Singh, T.P. (2020).
951 Structural and biochemical studies of phosphopantetheine adenylyltransferase from
952 *Acinetobacter baumannii* with dephospho-coenzyme A and coenzyme A. Int J Biol
953 Macromol *142*, 181-190. 10.1016/j.ijbiomac.2019.09.090.
954 45. Heath, R.J., and Rock, C.O. (1996). Inhibition of beta-ketoacyl-acyl carrier protein
955 synthase III (FabH) by acyl-acyl carrier protein in *Escherichia coli*. The Journal of
956 biological chemistry *271*, 10996-11000. 10.1074/jbc.271.18.10996.

957 46. Phong, W.Y., Lin, W., Rao, S.P., Dick, T., Alonso, S., and Pethe, K. (2013).
958 Characterization of phosphofructokinase activity in *Mycobacterium tuberculosis* reveals
959 that a functional glycolytic carbon flow is necessary to limit the accumulation of toxic
960 metabolic intermediates under hypoxia. PLoS One *8*, e56037.
961 10.1371/journal.pone.0056037.
962 47. Skarlatos, P., and Dahl, M.K. (1998). The glucose kinase of *Bacillus subtilis*. J Bacteriol
963 *180*, 3222-3226. 10.1128/JB.180.12.3222-3226.1998.
964 48. Boulanger, E.F., Sabag-Daigle, A., Thirugnanasambantham, P., Gopalan, V., and Ahmer,
965 B.M.M. (2021). Sugar-Phosphate Toxicities. Microbiol Mol Biol Rev *85*, e0012321.
966 10.1128/MMBR.00123-21.
967 49. Zeng, L., and Burne, R.A. (2021). Molecular mechanisms controlling fructose-specific
968 memory and catabolite repression in lactose metabolism by *Streptococcus mutans*. Mol
969 Microbiol *115*, 70-83. 10.1111/mmi.14597.
970 50. Morrissey, A.T., and Fraenkel, D.G. (1972). Suppressor of phosphofructokinase
971 mutations of *Escherichia coli*. J Bacteriol *112*, 183-187. 10.1128/jb.112.1.183-187.1972.
972 51. Babul, J. (1978). Phosphofructokinases from Escherichia coli. Purification and
973 characterization of the nonallosteric isozyme. The Journal of biological chemistry *253*,
974 4350-4355.
975 52. Deckers, B., Vercauteren, S., De Kock, V., Martin, C., Lazar, T., Herpels, P., Dewachter,
976 L., Verstraeten, N., Peeters, E., Ballet, S., et al. (2023). YbiB: a novel interactor of the
977 GTPase ObgE. Nucleic Acids Res *51*, 3420-3435. 10.1093/nar/gkad127.
978 53. Vidwans, S.J., Ireton, K., and Grossman, A.D. (1995). Possible role for the essential
979 GTP-binding protein Obg in regulating the initiation of sporulation in *Bacillus subtilis*. J
980 Bacteriol *177*, 3308-3311. 10.1128/jb.177.11.3308-3311.1995.
981 54. Okamoto, S., Itoh, M., and Ochi, K. (1997). Molecular cloning and characterization of
982 the obg gene of *Streptomyces griseus* in relation to the onset of morphological
983 differentiation. J Bacteriol *179*, 170-179. 10.1128/jb.179.1.170-179.1997.
984 55. Okamoto, S., and Ochi, K. (1998). An essential GTP-binding protein functions as a
985 regulator for differentiation in *Streptomyces coelicolor*. Mol Microbiol *30*, 107-119.
986 10.1046/j.1365-2958.1998.01042.x.
987 56. Verstraeten, N., Knapen, W.J., Kint, C.I., Liebens, V., Van den Bergh, B., Dewachter, L.,
988 Michiels, J.E., Fu, Q., David, C.C., Fierro, A.C., et al. (2015). Obg and Membrane
989 Depolarization Are Part of a Microbial Bet-Hedging Strategy that Leads to Antibiotic
990 Tolerance. Molecular cell *59*, 9-21. 10.1016/j.molcel.2015.05.011.
991 57. Feng, B., Mandava, C.S., Guo, Q., Wang, J., Cao, W., Li, N., Zhang, Y., Wang, Z., Wu,
992 J., Sanyal, S., et al. (2014). Structural and functional insights into the mode of action of a
993 universally conserved Obg GTPase. PLoS Biol *12*, e1001866.
994 10.1371/journal.pbio.1001866.
995 58. Murti, K.G., Webster, R.G., and Jones, I.M. (1988). Localization of RNA polymerases on
996 influenza viral ribonucleoproteins by immunogold labeling. Virology *164*, 562-566.
997 10.1016/0042-6822(88)90574-0.
998 59. Zielke, R., Sikora, A., Dutkiewicz, R., Wegrzyn, G., and Czyż, A. (2003). Involvement of
999 the cgtA gene function in stimulation of DNA repair in *Escherichia coli* and *Vibrio*
1000 *harveyi*. Microbiology (Reading) *149*, 1763-1770. 10.1099/mic.0.26292-0.
1001 60. Czyz, A., Zielke, R., Konopa, G., and Wegrzyn, G. (2001). A Vibrio harveyi insertional
1002 mutant in the *cgtA* (*obg*, *yhbZ*) gene, whose homologues are present in diverse organisms

1003 ranging from bacteria to humans and are essential genes in many bacterial species.
1004 Microbiology (Reading) *147*, 183-191. 10.1099/00221287-147-1-183.
1005 61. Courcelle, J., Khodursky, A., Peter, B., Brown, P.O., and Hanawalt, P.C. (2001).
1006 Comparative gene expression profiles following UV exposure in wild-type and SOS-
1007 deficient *Escherichia coli*. Genetics *158*, 41-64. 10.1093/genetics/158.1.41.
1008 62. Foti, J.J., Persky, N.S., Ferullo, D.J., and Lovett, S.T. (2007). Chromosome segregation
1009 control by *Escherichia coli* ObgE GTPase. Mol Microbiol *65*, 569-581. 10.1111/j.1365-
1010 2958.2007.05811.x.
1011 63. Tan, J., Jakob, U., and Bardwell, J.C. (2002). Overexpression of two different GTPases
1012 rescues a null mutation in a heat-induced rRNA methyltransferase. J Bacteriol *184*, 2692-
1013 2698. 10.1128/JB.184.10.2692-2698.2002.
1014 64. Nirody, J.A., Budin, I., and Rangamani, P. (2020). ATP synthase: Evolution, energetics,
1015 and membrane interactions. J Gen Physiol *152*. 10.1085/jgp.201912475.
1016 65. Lund, P., Tramonti, A., and De Biase, D. (2014). Coping with low pH: molecular
1017 strategies in neutralophilic bacteria. FEMS Microbiol Rev *38*, 1091-1125. 10.1111/1574-
1018 6976.12076.
1019 66. Wang, Y., Wu, J., Lv, M., Shao, Z., Hungwe, M., Wang, J., Bai, X., Xie, J., and Geng,
1020 W. (2021). Metabolism Characteristics of Lactic Acid Bacteria and the Expanding
1021 Applications in Food Industry. Front Bioeng Biotechnol *9*, 612285.
1022 10.3389/fbioe.2021.612285.
1023 67. Ajdic, D., McShan, W.M., McLaughlin, R.E., Savic, G., Chang, J., Carson, M.B.,
1024 Primeaux, C., Tian, R., Kenton, S., Jia, H., et al. (2002). Genome sequence of
1025 *Streptococcus mutans* UA159, a cariogenic dental pathogen. Proc Natl Acad Sci U S A
1026 *99*, 14434-14439. 10.1073/pnas.172501299.
1027 68. Peters, J.M., Colavin, A., Shi, H., Czarny, T.L., Larson, M.H., Wong, S., Hawkins, J.S.,
1028 Lu, C.H.S., Koo, B.M., Marta, E., et al. (2016). A Comprehensive, CRISPR-based
1029 Functional Analysis of Essential Genes in Bacteria. Cell *165*, 1493-1506.
1030 10.1016/j.cell.2016.05.003.
1031 69. Shields, R.C., Walker, A.R., Maricic, N., Chakraborty, B., Underhill, S.A.M., and Burne,
1032 R.A. (2020). Repurposing the *Streptococcus mutans* CRISPR-Cas9 System to Understand
1033 Essential Gene Function. PLoS Pathog *16*, e1008344. 10.1371/journal.ppat.1008344.
1034 70. Yother, J., Trieu-Cuot, P., Klaenhammer, T.R., and De Vos, W.M. (2002). Genetics of
1035 streptococci, lactococci, and enterococci: review of the sixth international conference. J
1036 Bacteriol *184*, 6085-6092. 10.1128/JB.184.22.6085-6092.2002.
1037 71. Otasek, D., Morris, J.H., Bouças, J., Pico, A.R., and Demchak, B. (2019). Cytoscape
1038 Automation: empowering workflow-based network analysis. Genome Biol *20*, 185.
1039 10.1186/s13059-019-1758-4.
1040
1041 **Figures and legends**
1042
1043 **Figure 1. Evolution of mutants deleted for essential genes in passage experiments.**
1044
1045 (a) Schematic representation of suppressor evolution when a mutant deleted for an essential gene
1046 is passaged multiple times. Shown is a replacement of a bacterial essential gene with the *kan*
1047 gene by homologous recombination through transformation. Secondary mutations conferring a
1048 fitness advantage become enriched in the population, and subsequent tertiary or quaternary

1049 mutations build upon the previously fixed mutations. Bold circles indicate cells, and colors of the
1050 bold circle indicate the development of cell lineages. Other symbols are defined in the figure.
1051
1052 (b) Two types of colonies, small and large, as demonstrated for *f1fo* deletion, appear on selection
1053 plates after 5 days of growth. Only the small colonies represent true deletions, denoted as Δ*f1fo*
1054 (red circle). The large colonies are "double-band mutants," containing both the replacement of
1055 the original *f1fo* with a *kan* gene and a wild-type *f1fo* copy, or they are mutants that did not
1056 contain a *kan* gene, but contained point mutations in other genes, denoted as Δ*f1fo-DB* (black
1057 circle, 'DB' for double-band).
1058
1059 (c) Incubation time (days) required for P0 and P6 mutants to reach an OD_{600} of 0.1 to 0.5.
1060
1061
1062
1063 **Figure 2. Identification of suppressors in mutants deleted for essential genes.**
1064
1065 (a) Number of independently evolved populations of different mutants.
1066
1067 (b-i) Evolved populations containing large-scale duplications. Red arrow, site of original
1068 essential gene deletion; Y axis indicates number of sequence reads mapped to the
1069 reference sequence at the coordinates shown on X axis.
1070
1071 (j) Boxplot of mutated segments (≥30% abundance) in the independently evolved populations of
1072 mutants deleted for essential genes or WT. Open circles indicate outliers.
1073
1074 (k) Stacked proportions of populations containing mutated segments comprising >50% (blue) or
1075 30%-50% (red) of sequence reads.
1076
1077 (l) Stacked proportions of mutated segments belonging to intergenic regions, non-essential
1078 ORFs, or essential ORFs.
1079
1080 (m) Stacked proportions of evolved populations with/without mutations in the multi-drug
1081 resistance genes (DRGs: *rpsL*, *gyrB*, *rpoB* and *rrs2*) shown.
1082
1083
1084 **Figure 3. Networks derived from the mutations in the evolved populations.**
1085
1086 **(a)** A network was built from the lists of suppressor mutants derived from each essential gene
1087 mutant and WT. Yellow-highlighted labels indicate the names of the essential genes mutated and
1088 the blue-highlighted label indicates the passaged WT. In total, there are twenty-five groups. Gene
1089 names without any marks, mutated segments belonging to essential genes; gene names with an
1090 asterisk (*) on the left, conditional essential genes; gene name with two asterisks on the left, non-
1091 essential genes; P_ followed by gene names and an asterisk, promoters; In_ followed by gene
1092 names and an asterisk and int_ followed by number, intergenic regions; _ followed by number,
1093 gene locus.
1094

1095 (b) Most commonly mutated segments in the evolved populations deleted of essential genes. Red
1096 cross on the rectangle boxes indicates evolved populations deleted of essential genes. Labels
1097 within the rectangle boxes indicate the segments with mutations. Numbers on top of the
1098 rectangle boxes indicate number of populations with mutations in the segments out of the total
1099 populations. Arrows indicate the flow of biochemical reactions.
1100
1101
1102 **Figure 4. Increasing *v1vo* copy number and inhibition of *trkA1-H1* independently**
1103 **contribute to the fitness improvement of evolved *Δf1fo* populations.**
1104
1105 (a) Gene duplication of *v1vo* region does not occur in P1 population (upper) and appeared in P6
1106 (lower) population of *Δf1fo#109.* Yellow arrows indicate passaging process. The black box
1107 indicates the *f1fo* region.
1108
1109 (b) Population of *Δf1fo#4* at P6 that does not contain gene duplication of *v1vo* region (upper).
1110 *v1vo* region duplication was observed in P15 (lower). (Two out of sixed evolved populations; see
1111 S7). Arrows indicate passaging process.
1112
1113 (c) *v1vo* region deleted in WT (upper). Duplication of *v1vo* region *Δf1fo#4, denoted as v1vo-DB/*
1114 *Δf1fo#4.* The black box indicates the *f1fo* region. The red box indicates *v1vo* region.
1115
1116 (d) Mutation frequency in *trkH1* increased with passage in P6 compared to P1 in population
1117 *Δf1f*#104.
1118
1119 (e) Growth of strains indicated. 0.1 OD_{600} of cells in a volume of 2 µl were spotted directly (first
1120 column) or diluted 20-fold (column 2), or 400-fold (column 3) and grown on BHI-agar for two
1121 days.
1122
1123 (f) Growth of the strains indicated. 0.1 OD_{600} of cells in a volume of 2 µl were spotted directly
1124 (first column) or diluted 10-fold (column 2), or 100-fold (column 3), or 1000-fold (column 4),
1125 and grown for four days.
1126
1127 (g) Quantitative growth measurements of WT, *ΔtrkA1-H1, ΔtrkA2-H2, Δf1fo* in *ΔtrkA1-H1* and
1128 *Δf1fo* in *ΔtrkA2-H2.* Culture is in BHI for 24 hr in anaerobic conditions. Data are shown as
1129 means ± SD from three replicate cultures. Different letters indicate statistically significant
1130 differences ($P \leq 0.05$), determined by one -way ANOVA with Tukey multiple comparisons test.
1131
1132 (h) Sensitivity of *Δf1fo#4* and WT to low pH (lactic acid: LA). The values are relative OD_{600} to
1133 that of WT grown in plain BHI. X-axis denotes the vol (µL) of 90% LA in 25 mL of BHI. Data
1134 are shown as means ± SD from three replicate cultures.
1135
1136 (i) Sensitivity of *Δf1fo#4* and WT to high pH (NaOH). The values are relative OD_{600} to that of
1137 WT grown in plain BHI. X-axis denotes the vol (µL) of 5 M NaOH in 25 mL of BHI. Data are
1138 shown as means ± SD from three replicate cultures.
1139
1140

1141
1142
1143 **Figure 5 Essentiality of *f1fo* in *S. mutans* UA159, *S. sanguinis* SK36, SK405 and SK1058.**
1144
1145 (a) Distribution of the genes indicated in *S. mutans* UA159, *S. sanguinis* SK36, SK405 and
1146 SK1058.
1147
1148 (b) Growth of *Δf1fo* transformants in *S. sanguinis* SK405 (upper) and SK1058 (lower) on same
1149 BHI agar medium for five days. Enlarged images of the transformants are shown. Red circles
1150 indicate small colonies, *Δf1fo*. Black circles indicate big colonies, *Δf1fo-DB*.
1151
1152 (c) Deletion of *f1fo* in SK405 or SK1058 shown by whole genome sequencing. Black box
1153 indicates the location of *f1fo* region.
1154
1155 (d) Quantitative measurements of growth in wild-type SK36, SK405 or SK1058, *ΔtrkA1-H1* or
1156 *Δf1fo* mutants in the backgrounds of SK36, SK405 or SK1058. Cells were grown in BHI for 24
1157 hours. Data are shown as means ± SD from three replicate cultures. Different letters indicate
1158 statistically significant differences ($P \leq 0.05$), determined by one -way ANOVA with Tukey
1159 multiple comparisons test.
1160
1161 (e) Growth of SK36, SK405 or SK1058, *ΔtrkA1-H1* mutant in the backgrounds of SK36, SK405
1162 or SK1058. 0.1 OD_{600} of cells in a volume of 2 µl were spotted directly (first column) or diluted
1163 10-fold (column 2), or 100-fold (column 3), or 1000-fold (column 4). Growth of Cells were
1164 grown on BHI-agar for two days.
1165
1166 (f) Growth of SK36, SK405 or SK1058, *Δf1fo* mutant in the backgrounds of SK36, SK405 or
1167 SK1058. Cells were diluted as in Fig. E and grown on BHI-agar for four days.
1168
1169 (g) Location of *trkA1-H1* suppressor mutations in SK405 and SK1058. Mutation of *trkA1-H1*
1170 appeared in all evolved *Δf1fo* populations, three in SK405 and two in SK1058. X-axis indicates
1171 the genome coordinates.
1172
1173
1174 **Supplemental Figures, Tables and legends**
1175
1176
1177 **Supplementary Fig.1. Genotyping and complementation of mutants deleted of *f1fo*.**
1178
1179 (a) Gene knockout strategy to delete entire region of eight *f1fo* subunits by homologous
1180 recombination. The yellow blocks indicate the eight F1Fo subunit genes in WT (upper). The blue
1181 block indicates the *kan* gene in Δ*f1fo* mutants (lower).
1182
1183 (b) Whole-genome sequencing to confirm the genotypes of the small colonies for Δ*f1fo* mutants.
1184 Black box indicates the location of deleted *f1fo* region. Enlarged image showed alignment of
1185 sequencing reads to the reference genome of *S. sanguinis* SK36. The blue graphic above the

sequence coordinates (indicated by a red arrow) indicates the extent of coverage, the yellow bars indicate the mismatches, and the bracket indicates the aligned sequence reads.

(c) Whole-genome sequencing of the big colonies, Δ*f1fo*-DB. Black box indicates the location of *f1fo* region. Red arrows indicate the two directly repeated *ugpC* genes, encoding glycerol-3-phosphate ABC transporter.

Supplementary Fig.2. Isolation of viable mutants deleted essential genes and genotyping by whole-genome sequencing.

(a-b) Colonies of transformants (left) and whole-genome sequencing of colonies (right). Red circles indicate the colonies picked for whole-genome sequencing (left). For genome sequencing (right), the blue graphic above the sequence coordinates (indicated by a red arrow in the top panel of a.1) indicates the extent of coverage, the yellow bars indicate the mismatches, and the bracket indicates the aligned sequence reads. Bacterial colonies on selective agar plate for five days. (a.1-a.2) Gene deletion mutants with severe growth defects. (b) Gene deletion mutants with robust growth. Scale bar: 1 mm. The image of Δ*f1fo* transformation is a duplicate of Figure 1B to demonstrate the transformants in selection medium Δ*f1fo* alignment is a duplication of Fig.S1c.

Supplementary Fig.3. Growth of mutants deleted of essential genes, relative to that of WT.

(a-b) Growth mutants deleted of 23 essential genes under anaerobic condition (a) and microaerobic condition (b). 0.1 OD_{600} of cells in a volume of 2 µl were spotted directly (first column) or diluted 20-fold (column 2), or 400-fold (column 3) and grown on BHI-agar for two days. Scale bar is 1 cm.

(c) Comparison of the growth of the twenty-four evolved mutants and that of WT. The values are relative OD_{600} after 24 hr of growth in BHI liquid medium for 24 hours.

Supplementary Fig.4. Large scale gene duplication present in the evolved populations of the mutants deleted essential genes but not in WT populations.

(a) Whole-genome sequencing of parental WT and the six evolved WT populations after nine passages. The yellow arrow indicates the passage procedure.

(b-e) Evolved populations that contain gene duplication of greater than 10 kb in Δ*uncE#3* (b), Δ*f1fo#107* (c), Δ*fabH#4* (d) *and* Δ*fabH#6* (e). Red arrows (b-e) indicate the location of the gene intentionally deleted. The insert image (c) is an enlarged segments of *uncE* region, shown as a black box.

Supplementary Fig.S5. Appearance of mutations in essential genes in the evolved populations of strains intentionally deleted for different essential genes.

1232
1233 (a-f) Aligned sequence reads from *ΔuncC#1* of P1 population (a-c) and P6 population (d-f). Red
1234 arrows indicate the deleted *uncC* in the genome (a and d) in the *ΔuncC#1* strain. Red box
1235 indicates mutation of *uncH* in *ΔuncC#1* (a and d). Enlarged mutated *uncH* region of aligned
1236 sequence reads in *ΔuncC#1* of P1 population (b-c) and P6 population (e-f). The yellow arrow
1237 indicates the passage procedure.
1238
1239 (g) Sequencing of the mutated *uncH* gene in *ΔuncC#1* in P6. Red letters indicate a fragment (82
1240 bp) that was present in mutated *uncH* gene (upper). Asterisk (*) indicates the stop codon that was
1241 highlighted. Vertical bars indicate the coordinates of the *uncH* ORF (lower). The coordinates
1242 between two red bars indicate replaced region.
1243
1244 (h-k) Aligned sequence reads from *Δf1fo#107* of P1 population (h-i) and P6 population (j-k). Red
1245 arrows indicate the deleted *f1fo* in the genome (h and j) in the *Δf1fo#107*. Red box indicates
1246 mutation of *ftsZ* in *Δf1fo#107* (h and j). Enlarged mutated *ftsZ* region of aligned sequence reads
1247 in *Δf1fo#107* of P1 population (h) and P6 population (i). The yellow arrow indicates the passage
1248 procedure. Supplementary Fig.5J is a duplicate of Supplementary Fig.4B to show a genome
1249 alignment of *Δf1fo#107* of P6.
1250
1251 (l) Sequencing of the mutated *ftsZ* in *Δf1fo#107* in P6. Red letters indicate a fragment (248 bp)
1252 that was present in mutated *Δf1fo#107* (upper). Asterisk (*) indicates the stop codon that was
1253 highlighted. Vertical bars indicated the coordinates of the *uncH* ORF (lower). The red bar
1254 indicates the coordinate where insertion occurred.
1255
1256
1257 **Supplementary Fig.6. Populations with and without mutations in three PTS**
1258 **mannose/fructose/sorbose transporter subunits.**
1259
1260 (a-b) Number (a) and percentage (b) of populations that have mutations in any of three PTS
1261 mannose/fructose/sorbose transporter subunits, namely J1C87_09355, J1C87_09360, and
1262 J1C87_09365.
1263
1264 **Supplementary Fig.7. The most frequent suppressors identified in mutants deleted of**
1265 **essential genes.**
1266 The percentage of mutated segments in evolved populations in *Δf1fo*, mutants deleted of single
1267 *unc* subunit genes, denoted as *Δf1fo.s*, the other single mutants indicated, and WT. The names
1268 with an asterisk (*) indicate the intergenic regions.
1269
1270
1271 **Supplementary Fig.8. Appearance of *v1vo* region gene duplication during passage. (Related**
1272 **to Figure 4a and 4b)**
1273
1274 (a-b) Alignment of sequence reads in populations of *Δf1fo#107, Δf1fo#109, uncE#2* and *uncH#7*
1275 at P1 (A) and P6 (B). The black box indicates the deleted *f1fo* region and the red arrows indicate
1276 the deleted *uncE* or *uncH.*
1277

1278 (c) Alignment of sequence reads of the P6 population in *Δf1fo#4* (upper) and five derived
1279 populations from P15 (lower). Rectangles represent the deleted *f1fo* region. Asterisks (*) indicate
1280 the two populations with *v1vo* region gene duplications.
1281
1282
1283 **Supplementary Fig.9. Gene duplication in *Δv1vo-DB/Δf1fo#4* populations (related to Figure**
1284 **4c).**
1285
1286 Alignment of sequence reads of five additional *Δv1vo-DB/Δf1fo#4* populations. The black box
1287 indicates the deleted *f1fo*. The red box indicates the gene duplication of *v1vo* region when one
1288 copy of *v1vo* was deleted.
1289
1290
1291 **Supplementary Fig.10. Alignment of sequence reads of *trk* mutants with and without *f1fo***
1292 **deletion**.
1293
1294 (a-k) Alignment of sequence reads of *ΔtrkA1* (a), *ΔtrkH1* (b), *ΔtrkA1-H1* (c), *ΔtrkA2* (d), *ΔtrkH2*
1295 (e), *ΔtrkA2-H2* (f), *ΔtrkA1/ΔtrkH2* (g), *ΔtrkH1/ΔtrkH2* (h), *ΔtrkA1-H1/ΔtrkH2* (i), *Δf1fo/ΔtrkA1-*
1296 *H1* (j), and *Δf1fo/ΔtrkA2-H2* (k). Red arrows indicated intended gene deletion. The block box
1297 indicates the deleted *f1fo region.* (related to Figure 4f).
1298
1299 **Supplementary Fig.11. Working model for F1Fo, V1Vo, TrkA1-H1 and TrkA2-H2.**
1300
1301 For streptococci, which do not contain a complete tricarboxylic acid cycle (TCA: shaded) or
1302 electron transport chain (ETC: shaded), energy production is mainly through lactic acid
1303 fermentation. The lactate from fermentation creates acidic conditions in the cytosol, which
1304 becomes toxic if H+ is not exported. F1Fo pumps out H+ from the cytosol using ATP, and V1Vo
1305 supplements or replaces the function of F1Fo when the F1Fo is inhibited/inactivated. Both
1306 TrkA1-H1 and TrkA2-H1 are potassium transporters, and functionally redundant. TrkA1-H1
1307 pumps in potassium together with H+, acidifying the cytosol when H+ is not exported. In
1308 contrast, TrkA2-H2 does not pump protons into the cytosol when pumping in potassium (likely
1309 instead pumping in Na+). Therefore, the function of TrkA1-H1 must be inhibited if F1Fo is not
1310 functional. Solid lines indicate presence of reactions. Dashed lines indicate absence of reactions.
1311
1312 **Supplementary Fig.12. *f1fo* cannot be deleted in *S. mutans* UA159.**
1313
1314 (a) Gene knockout strategy to delete entire region of eight *f1fo* subunits by homologous
1315 recombination. The purple blocks indicate the eight F1Fo subunit genes in WT (upper). The blue
1316 block indicates the *kan* gene in Δ*f1fo* mutants (lower). The two arrows indicate the primer set for
1317 the PCR amplicon of the region in (B).
1318
1319 (b) Genotyping the presence of wild-type *f1fo* colonies from selection medium. P: positive
1320 control using DNA template from wild-type. N: negative control using water as a template. The
1321 size of amplicons is about 1300 bp.
1322
1323

1324 **Supplementary Fig.13. Deletion *of trkA1-H1* in *S. sanguinis* SK1058 and S. sanguinis**
1325 **SK405 (related to Figure 5c).**
1326
1327 (a-b) Alignment of sequence reads of *ΔtrkA1-H1* populations in SK405 (a) and in SK1058 (b)
1328 backgrounds.
1329
1330
1331 **Supplementary Fig.14. Deletion *of f1fo* in *S. sanguinis* SK1058 and SK405 (related to**
1332 **Figure 5c).**
1333 Alignment of sequence reads of three *Δf1fo* populations in SK405 backgrounds (a) and two in
1334 SK1058 backgrounds (b) (related to Figure 5c). Rectangles represent the deleted *f1fo* region.

Fig.1

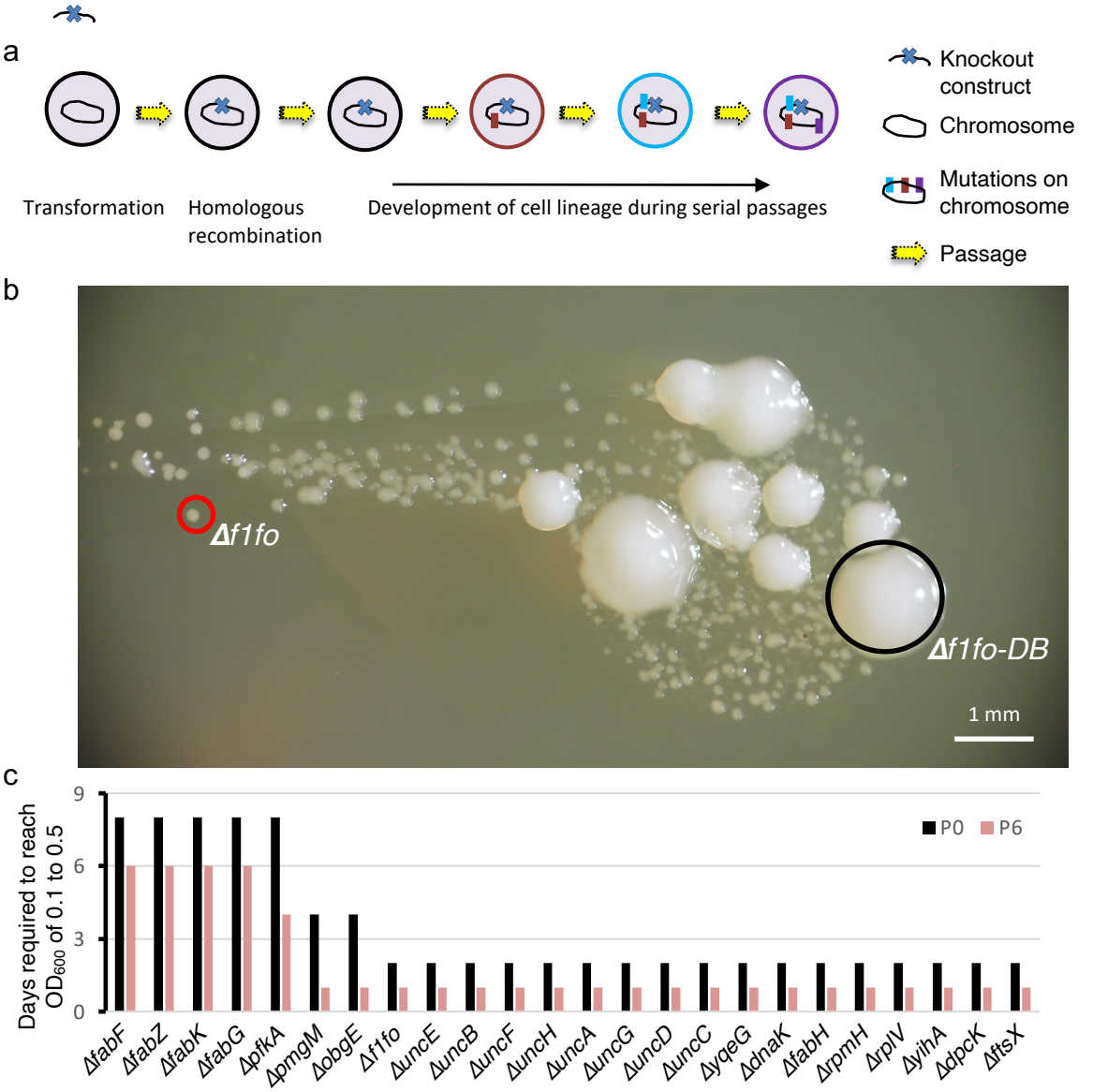
a
Knockout construct
Chromosome
Mutations on chromosome
Passage
Transformation
Homologous recombination
Development of cell lineage during serial passages
b
Δf1fo
Δf1fo-DB
1 mm
c
Days required to reach OD600 of 0.1 to 0.5
9
6
3
0
P0
P6
ΔfabF
ΔfabZ
ΔfabK
ΔfabG
ΔpfkA
ΔpmgM
ΔobgE
Δf1fo
ΔuncE
ΔuncB
ΔuncF
ΔuncH
ΔuncA
ΔuncG
ΔuncD
ΔuncC
ΔyqeG
ΔdnaK
ΔfabH
ΔrpmH
ΔrplV
ΔyihA
ΔdpcK
ΔftsX

Fig.2

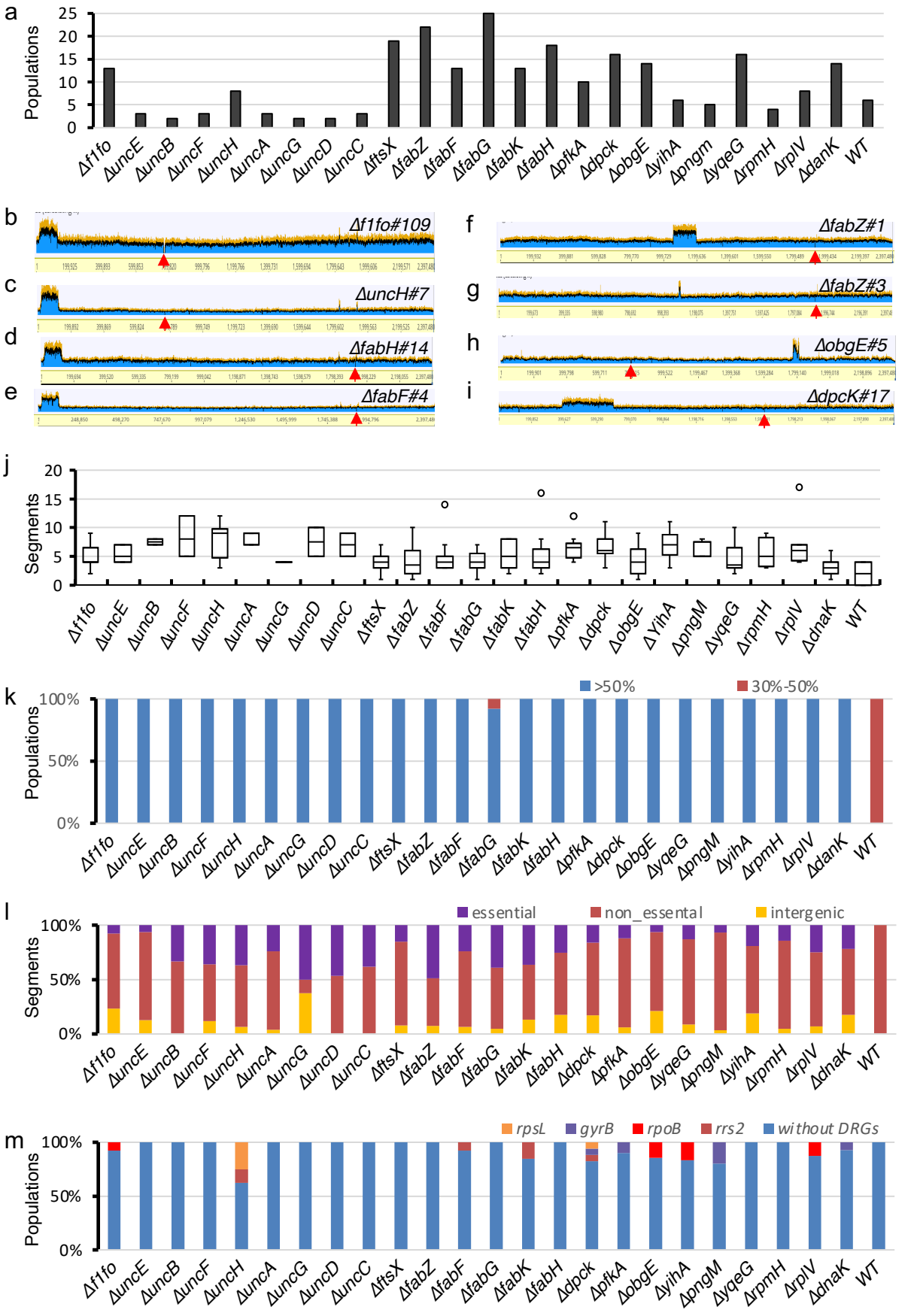
a
Populations
25
20
15
10
5
0
Δf1fo
ΔuncE
ΔuncB
ΔuncF
ΔuncH
ΔuncA
ΔuncG
ΔuncD
ΔuncC
ΔftsX
ΔfabZ
ΔfabF
ΔfabG
ΔfabK
ΔfabH
ΔpfkA
Δdpck
ΔobgE
ΔyihA
Δpngm
ΔyqeG
ΔrpmH
ΔrplV
ΔdanK
WT
b
Δf1fo#109
c
ΔuncH#7
d
ΔfabH#14
e
ΔfabF#4
f
ΔfabZ#1
g
ΔfabZ#3
h
ΔobgE#5
i
ΔdpcK#17
j
Segments
20
15
10
5
0
Δf1fo
ΔuncE
ΔuncB
ΔuncF
ΔuncH
ΔuncA
ΔuncG
ΔuncD
ΔuncC
ΔftsX
ΔfabZ
ΔfabF
ΔfabG
ΔfabK
ΔfabH
ΔpfkA
Δdpck
ΔobgE
Δ YihA
ΔpngM
ΔyqeG
ΔrpmH
ΔrplV
ΔdnaK
WT
k
>50%
30%-50%
Populations
100%
50%
0%
Δf1fo
ΔuncE
ΔuncB
ΔuncF
ΔuncH
ΔuncA
ΔuncG
ΔuncD
ΔuncC
ΔftsX
ΔfabZ
ΔfabF
ΔfabG
ΔfabK
ΔfabH
ΔpfkA
Δdpck
ΔobgE
ΔyqeG
ΔpngM
ΔyihA
ΔrpmH
ΔrplV
ΔdanK
WT
l
essential
non_essental
intergenic
Segments
100%
50%
0%
Δf1fo
ΔuncE
ΔuncB
ΔuncF
ΔuncH
ΔuncA
ΔuncG
ΔuncD
ΔuncC
ΔftsX
ΔfabZ
ΔfabF
ΔfabG
ΔfabK
ΔfabH
Δdpck
ΔpfkA
ΔobgE
ΔyqeG
ΔpngM
ΔyihA
ΔrpmH
ΔrplV
ΔdnaK
WT
m
rpsL
gyrB
rpoB
rrs2
without DRGs
Populations
100%
50%
0%
Δf1fo
ΔuncE
ΔuncB
ΔuncF
ΔuncH
ΔuncA
ΔuncG
ΔuncD
ΔuncC
ΔftsX
ΔfabZ
ΔfabF
ΔfabG
ΔfabK
ΔfabH
Δdpck
ΔpfkA
ΔobgE
ΔyihA
ΔpngM
ΔyqeG
ΔrpmH
ΔrplV
ΔdnaK
WT

Fig.3

a

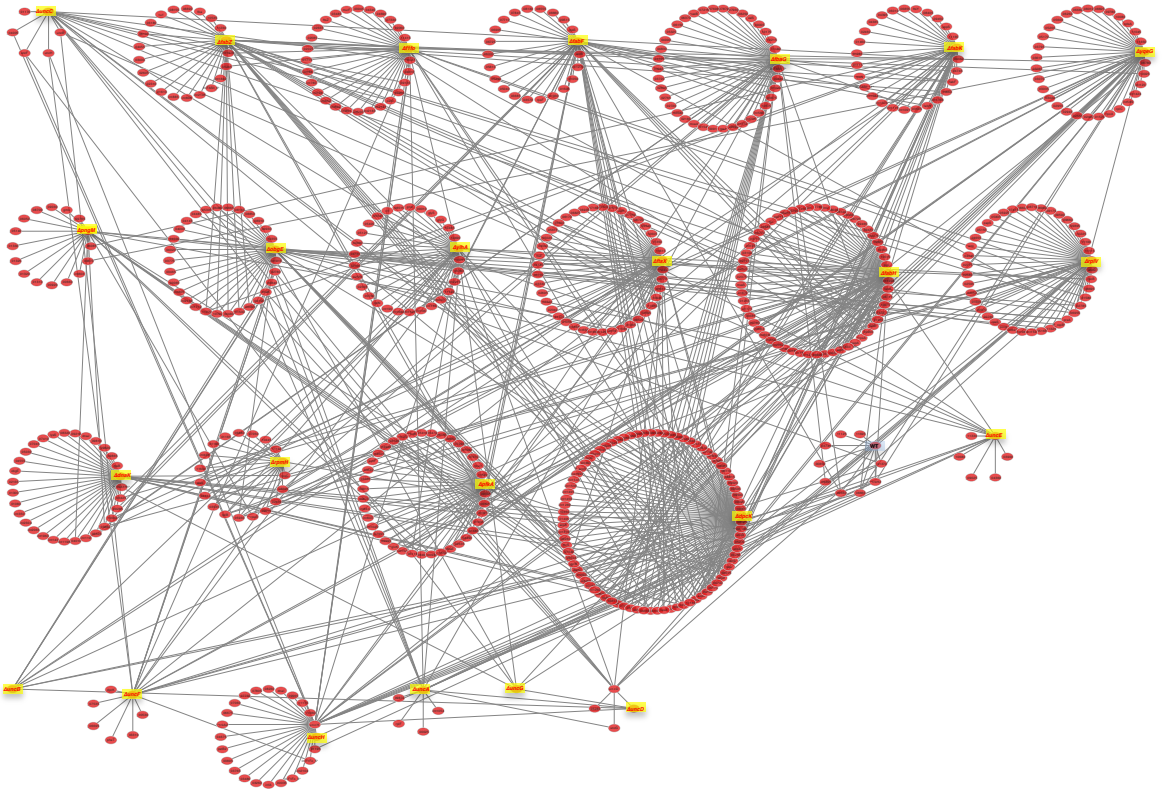

b

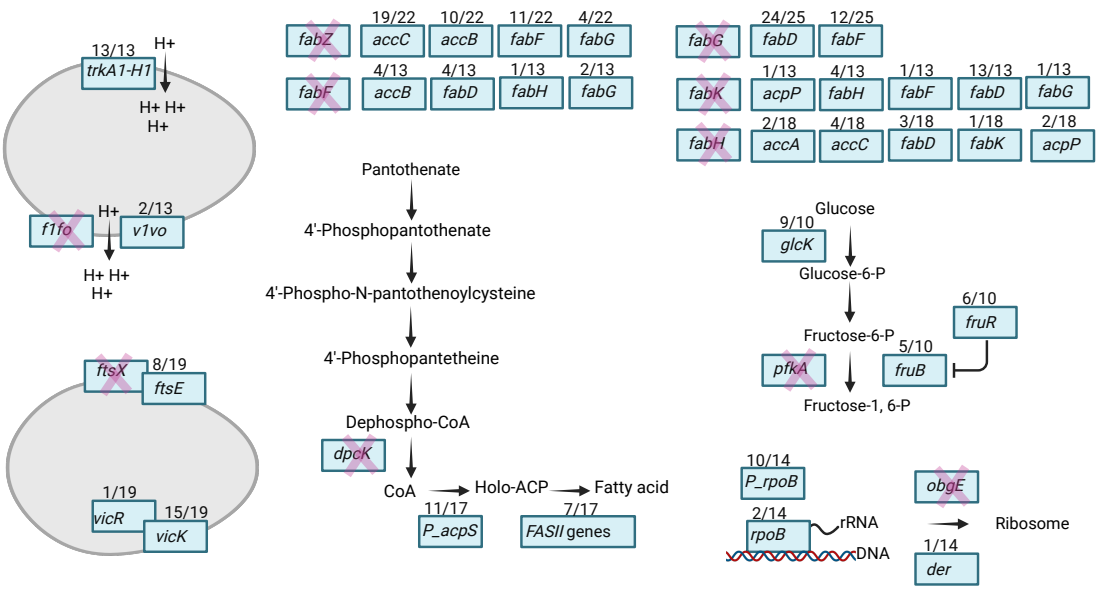
13/13
trkA1-H1
H+
H+ H+
H+
f1fo
H+
2/13
v1vo
H+ H+
H+
ftsX
8/19
ftsE
1/19
vicR
15/19
vicK
19/22
fabZ
accC
10/22
accB
11/22
fabF
4/22
fabG
fabF
4/13
accB
4/13
fabD
1/13
fabH
2/13
fabG
Pantothenate
4'-Phosphopantothenate
4'-Phospho-N-pantothenoylcysteine
4'-Phosphopantetheine
Dephospho-CoA
dpcK
CoA
Holo-ACP
Fatty acid
11/17
P_acpS
7/17
FASII genes
24/25
fabG
fabD
12/25
fabF
fabK
1/13
acpP
4/13
fabH
1/13
fabF
13/13
fabD
1/13
fabG
fabH
2/18
accA
4/18
accC
3/18
fabD
1/18
fabK
2/18
acpP
Glucose
9/10
glcK
Glucose-6-P
6/10
fruR
Fructose-6-P
5/10
fruB
pfkA
Fructose-1, 6-P
10/14
P_rpoB
2/14
rpoB
rRNA
DNA
obgE
Ribosome
1/14
der

Fig.4

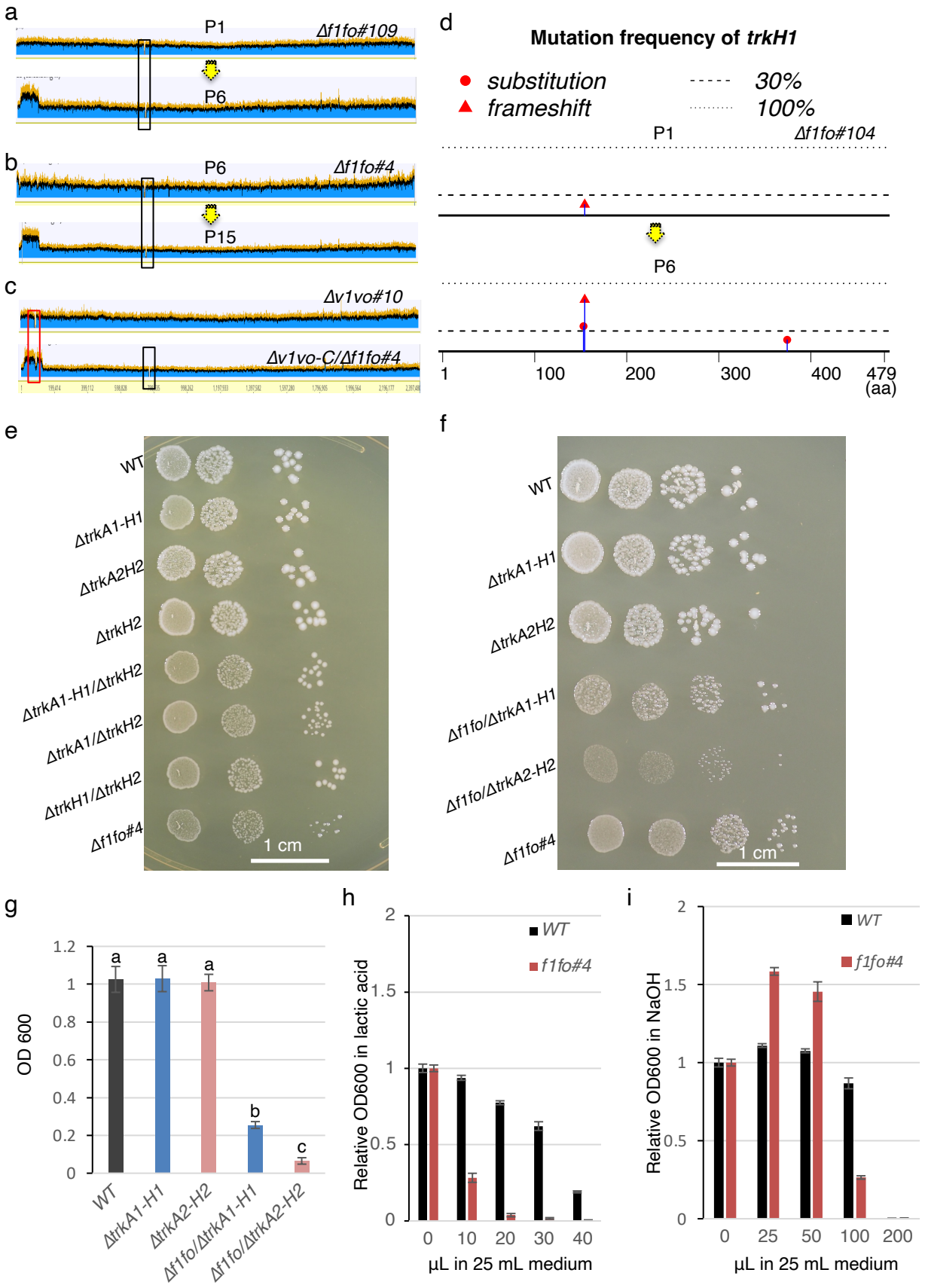
a
P1
Δf1fo#109
P6
b
P6
Δf1fo#4
P15
c
Δv1vo#10
Δv1vo-C/Δf1fo#4
d
Mutation frequency of trkH1
substitution
frameshift
30%
100%
P1
Δf1fo#104
P6
1
100
200
300
400
479
(aa)
e
WT
ΔtrkA1-H1
ΔtrkA2H2
ΔtrkH2
ΔtrkA1-H1/ΔtrkH2
ΔtrkA1/ΔtrkH2
ΔtrkH1/ΔtrkH2
Δf1fo#4
1 cm
f
WT
ΔtrkA1-H1
ΔtrkA2H2
Δf1fo/ΔtrkA1-H1
Δf1fo/ΔtrkA2-H2
Δf1fo#4
1 cm
g
OD 600
1.2
1
0.8
0.6
0.4
0.2
0
a
a
a
b
c
WT
ΔtrkA1-H1
ΔtrkA2-H2
Δf1fo/ΔtrkA1-H1
Δf1fo/ΔtrkA2-H2
h
Relative OD600 in lactic acid
2
1.5
1
0.5
0
WT
f1fo#4
0
10
20
30
40
μL in 25 mL medium
i
Relative OD600 in NaOH
2
1.5
1
0.5
0
WT
f1fo#4
0
25
50
100
200
μL in 25 mL medium

Fig.5

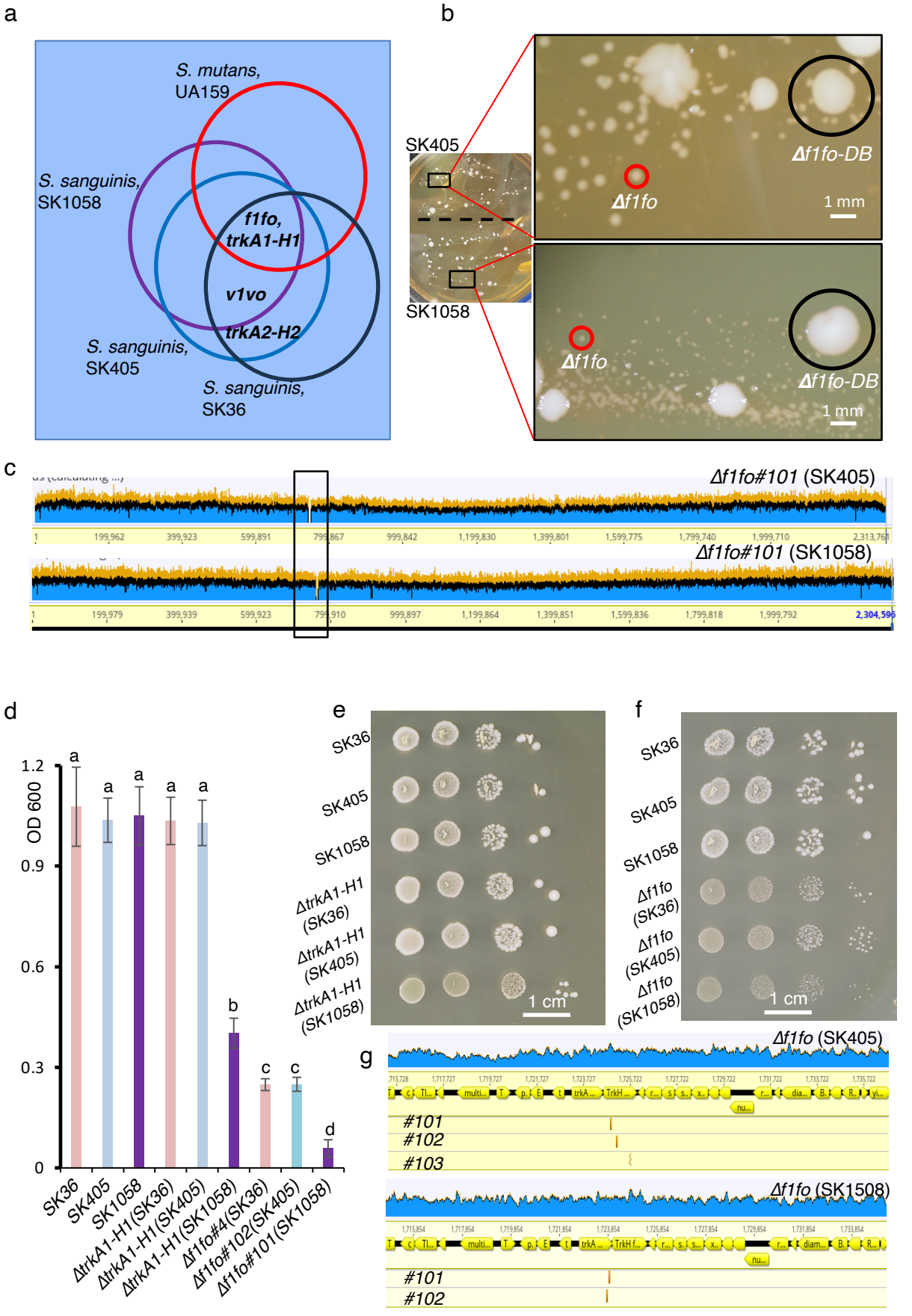
a
S. mutans, UA159
S. sanguinis, SK1058
f1fo, trkA1-H1
v1vo
trkA2-H2
S. sanguinis, SK405
S. sanguinis, SK36
b
SK405
SK1058
Δf1fo-DB
Δf1fo
1 mm
c
Δf1fo#101 (SK405)
Δf1fo#101 (SK1058)
d
OD 600
SK36
SK405
SK1058
ΔtrkA1-H1(SK36)
ΔtrkA1-H1(SK405)
ΔtrkA1-H1(SK1058)
Δf1fo#4(SK36)
Δf1fo#102(SK405)
Δf1fo#101(SK1058)
e
1 cm
f
1 cm
g
Δf1fo (SK405)
#101
#102
#103
Δf1fo (SK1508)
#101
#102

Fig S1

a

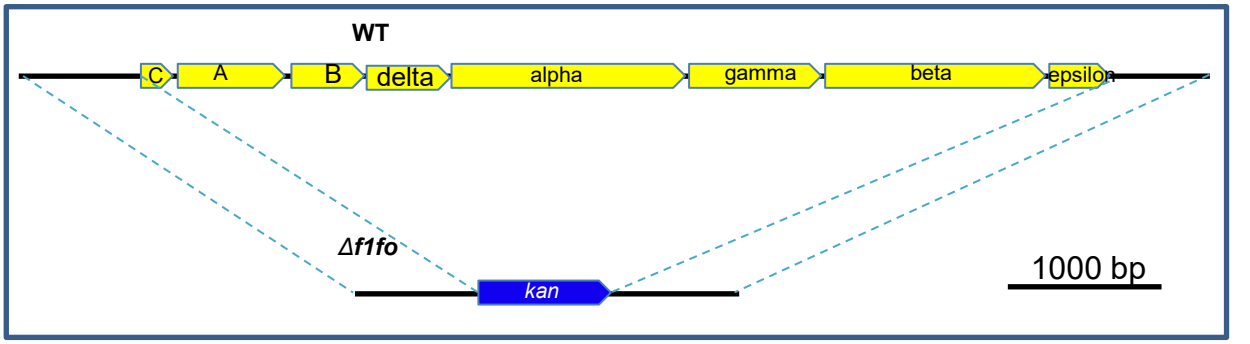
WT
C
A
B
delta
alpha
gamma
beta
epsilon
Δf1fo
kan
1000 bp

b

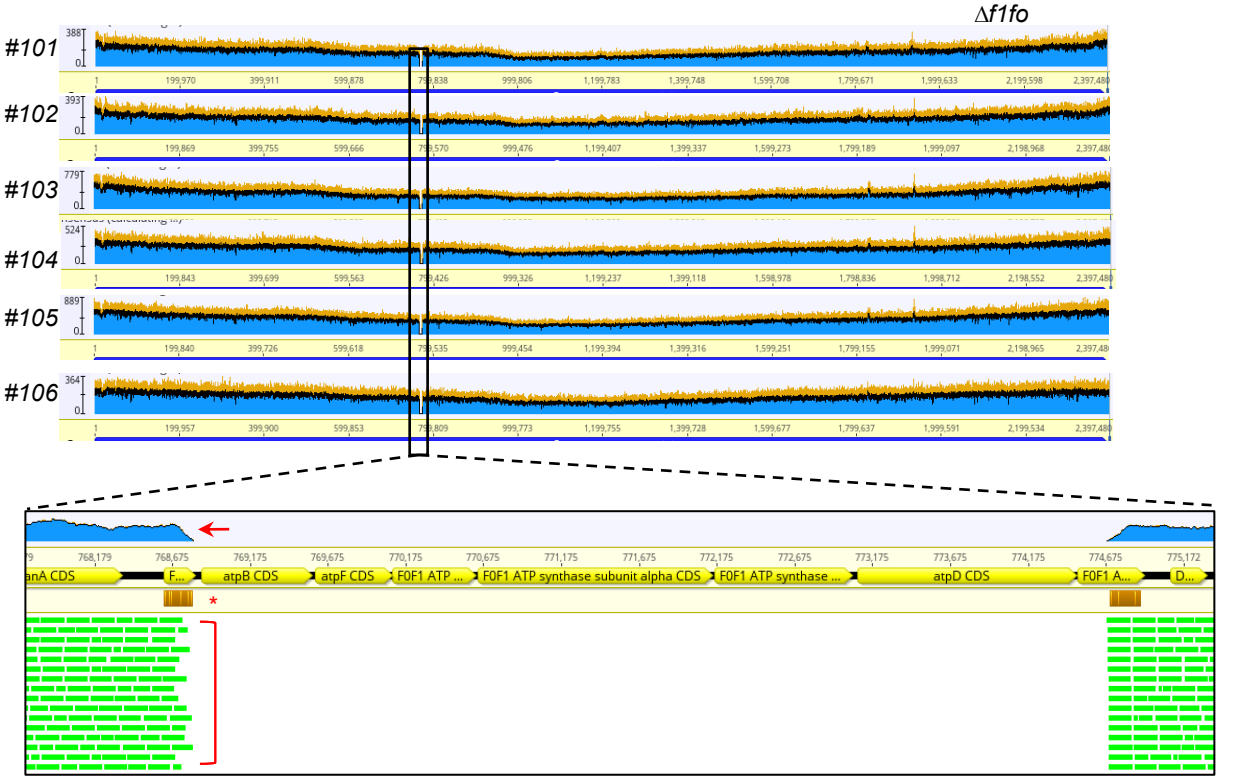
Δf1fo
#101
#102
#103
#104
#105
#106
anA CDS
F...
atpB CDS
atpF CDS
F0F1 ATP ...
F0F1 ATP synthase subunit alpha CDS
F0F1 ATP synthase ...
atpD CDS
F0F1 A...
D...
*

c

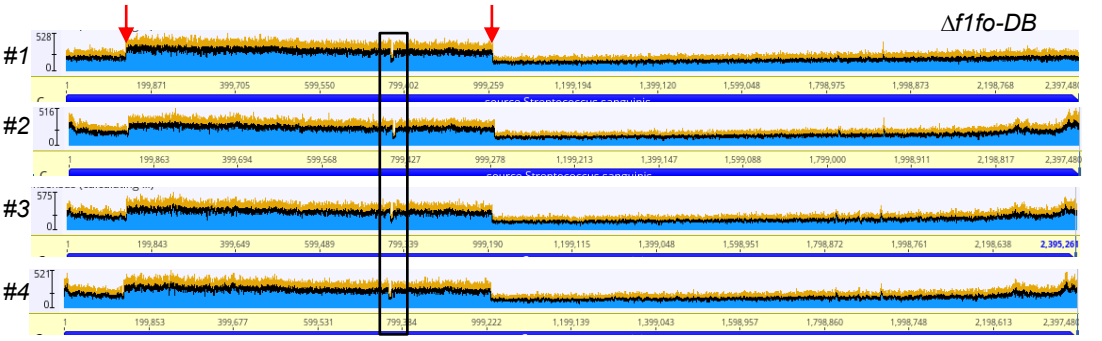
Δf1fo-DB
#1
#2
#3
#4

Fig S2

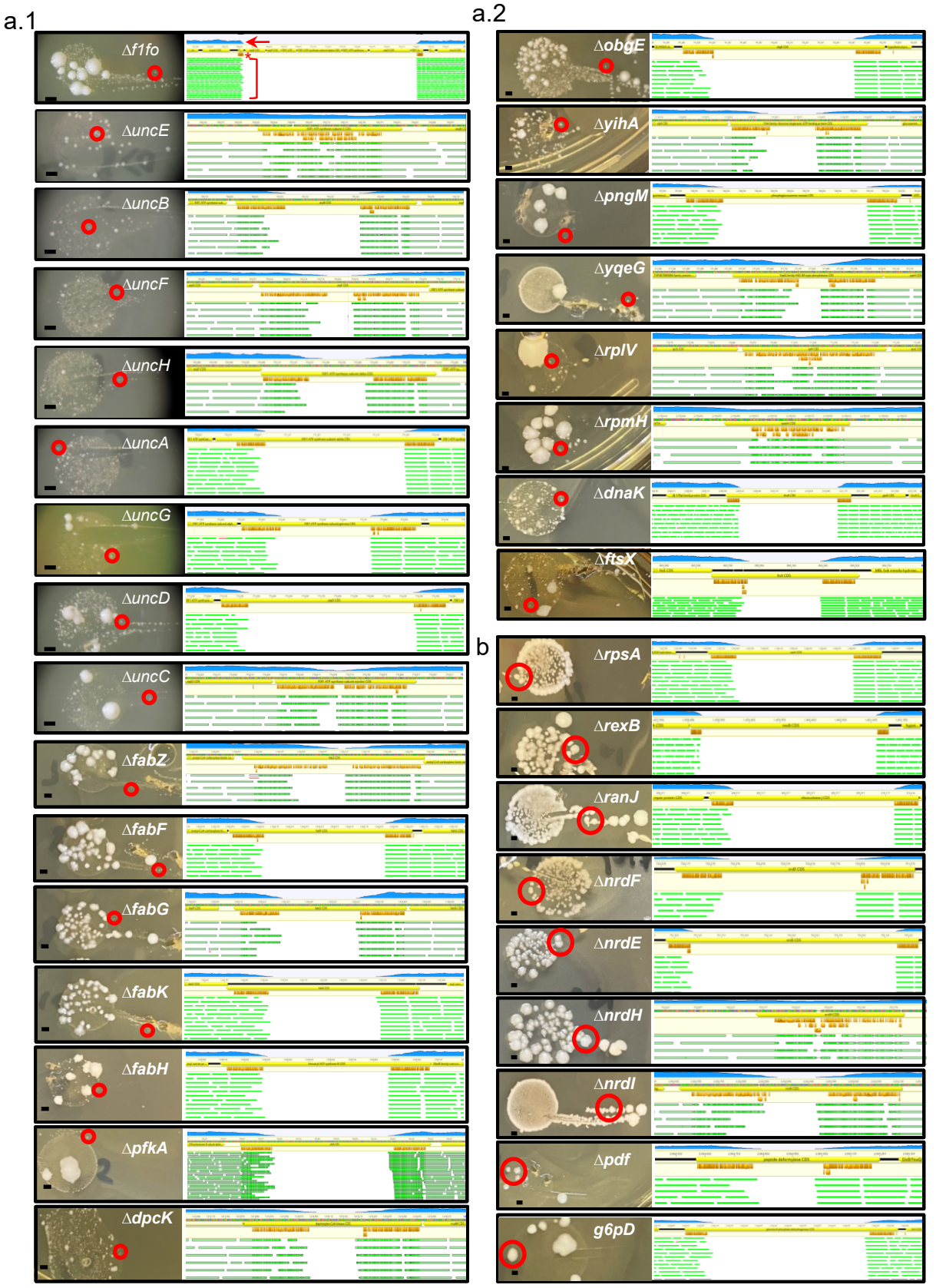
a.1
Δf1fo
ΔuncE
ΔuncB
ΔuncF
ΔuncH
ΔuncA
ΔuncG
ΔuncD
ΔuncC
ΔfabZ
ΔfabF
ΔfabG
ΔfabK
ΔfabH
ΔpfkA
ΔdpcK
a.2
ΔobgE
ΔyihA
ΔpngM
ΔyqeG
ΔrplV
ΔrpmH
ΔdnaK
ΔftsX
b
ΔrpsA
ΔrexB
ΔranJ
ΔnrdF
ΔnrdE
ΔnrdH
ΔnrdI
Δpdf
g6pD

Fig S3

a

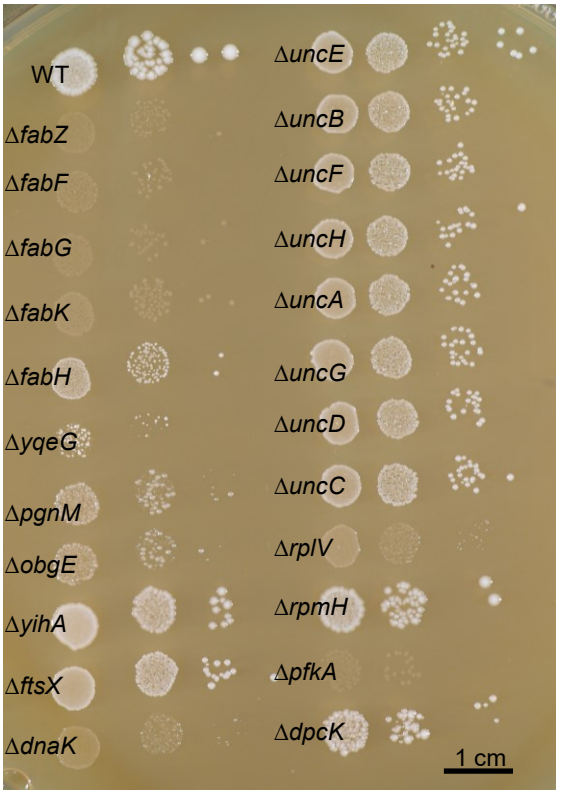
WT
ΔfabZ
ΔfabF
ΔfabG
ΔfabK
ΔfabH
ΔyqeG
ΔpgnM
ΔobgE
ΔyihA
ΔftsX
ΔdnaK
ΔuncE
ΔuncB
ΔuncF
ΔuncH
ΔuncA
ΔuncG
ΔuncD
ΔuncC
ΔrplV
ΔrpmH
ΔpfkA
ΔdpcK
1 cm

b

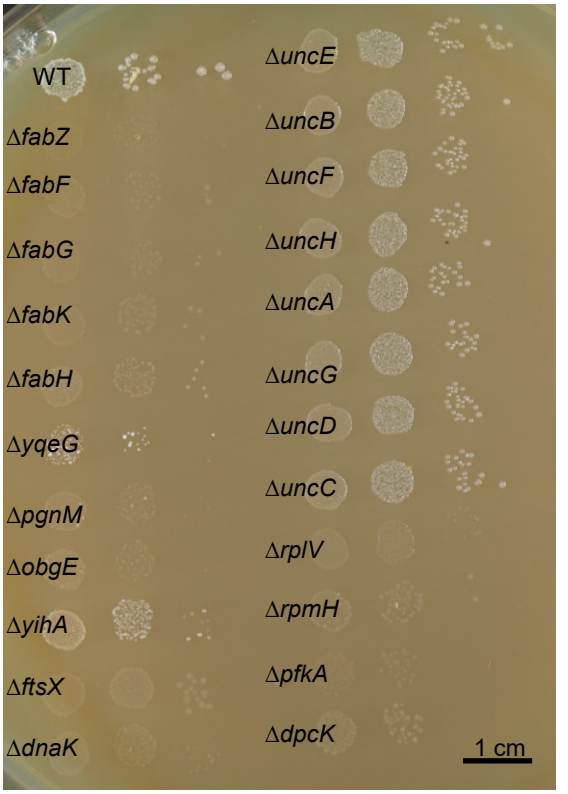
WT
ΔfabZ
ΔfabF
ΔfabG
ΔfabK
ΔfabH
ΔyqeG
ΔpgnM
ΔobgE
ΔyihA
ΔftsX
ΔdnaK
ΔuncE
ΔuncB
ΔuncF
ΔuncH
ΔuncA
ΔuncG
ΔuncD
ΔuncC
ΔrplV
ΔrpmH
ΔpfkA
ΔdpcK
1 cm

c

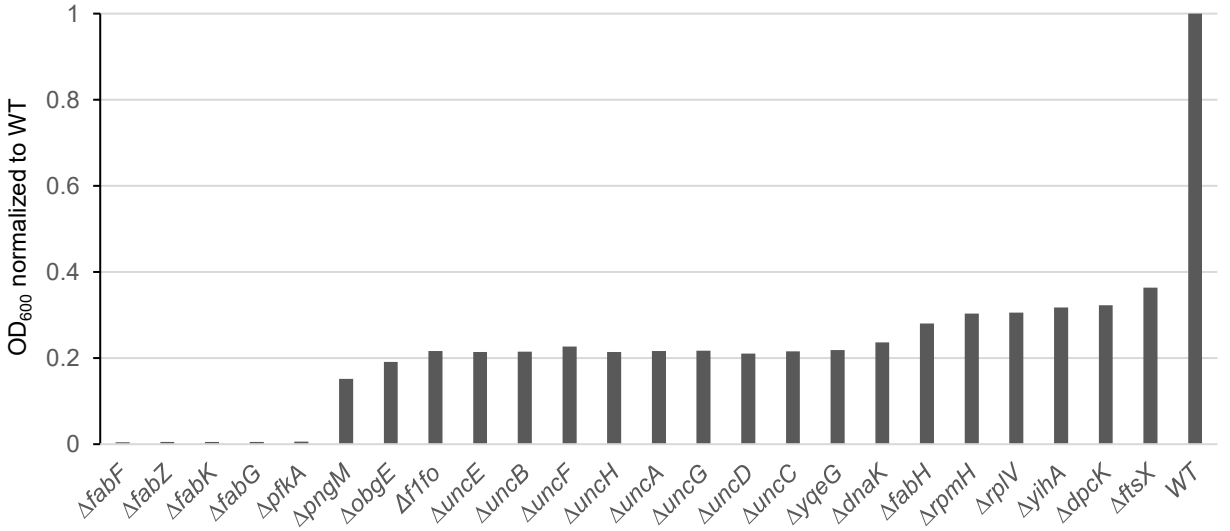
OD600 normalized to WT
1
0.8
0.6
0.4
0.2
0
ΔfabF
ΔfabZ
ΔfabK
ΔfabG
ΔpfkA
ΔpngM
ΔobgE
Δf1fo
ΔuncE
ΔuncB
ΔuncF
ΔuncH
ΔuncA
ΔuncG
ΔuncD
ΔuncC
ΔyqeG
ΔdnaK
ΔfabH
ΔrpmH
ΔrplV
ΔyihA
ΔdpcK
ΔftsX
WT

Fig S4

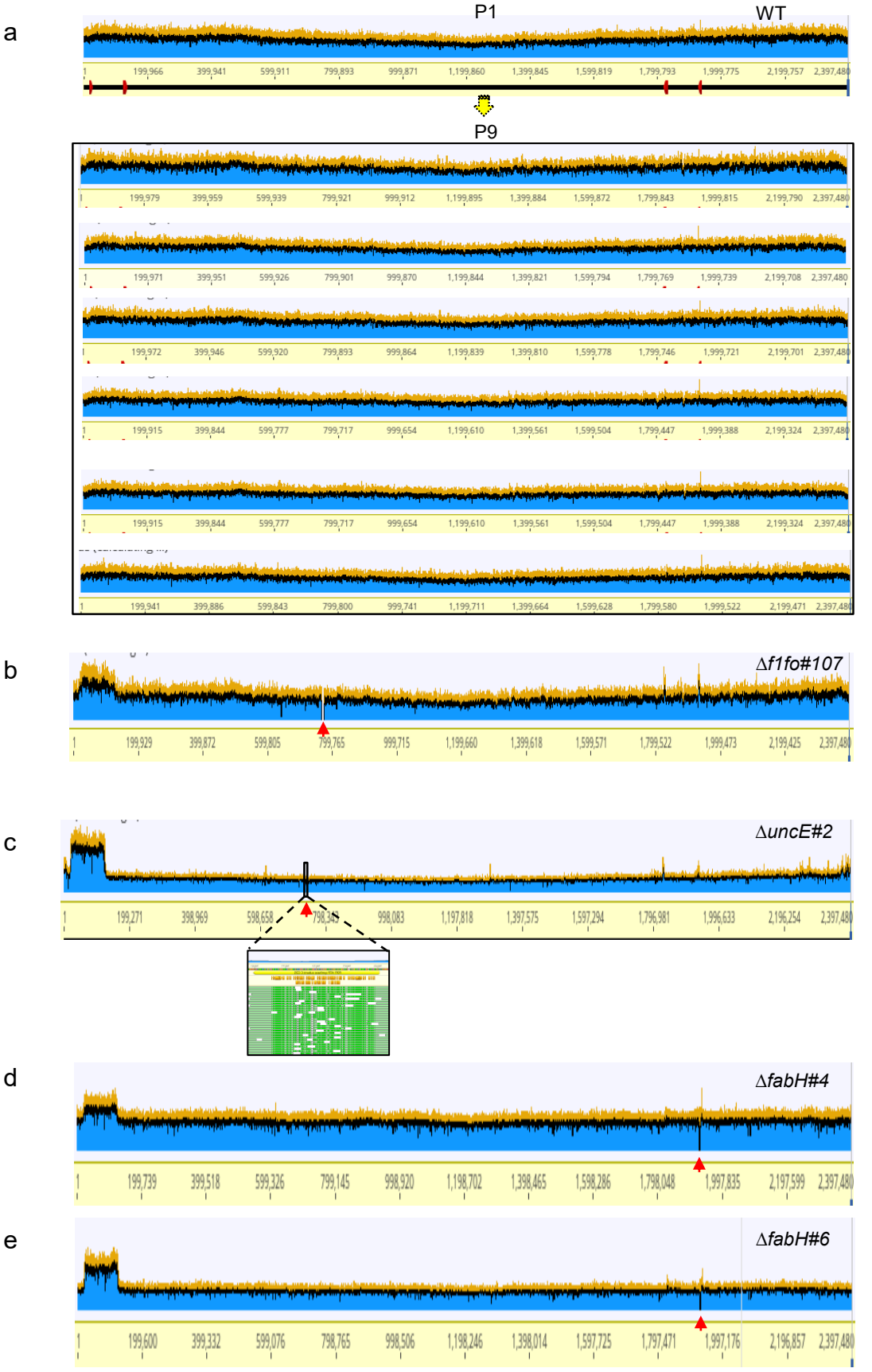

Fig S5

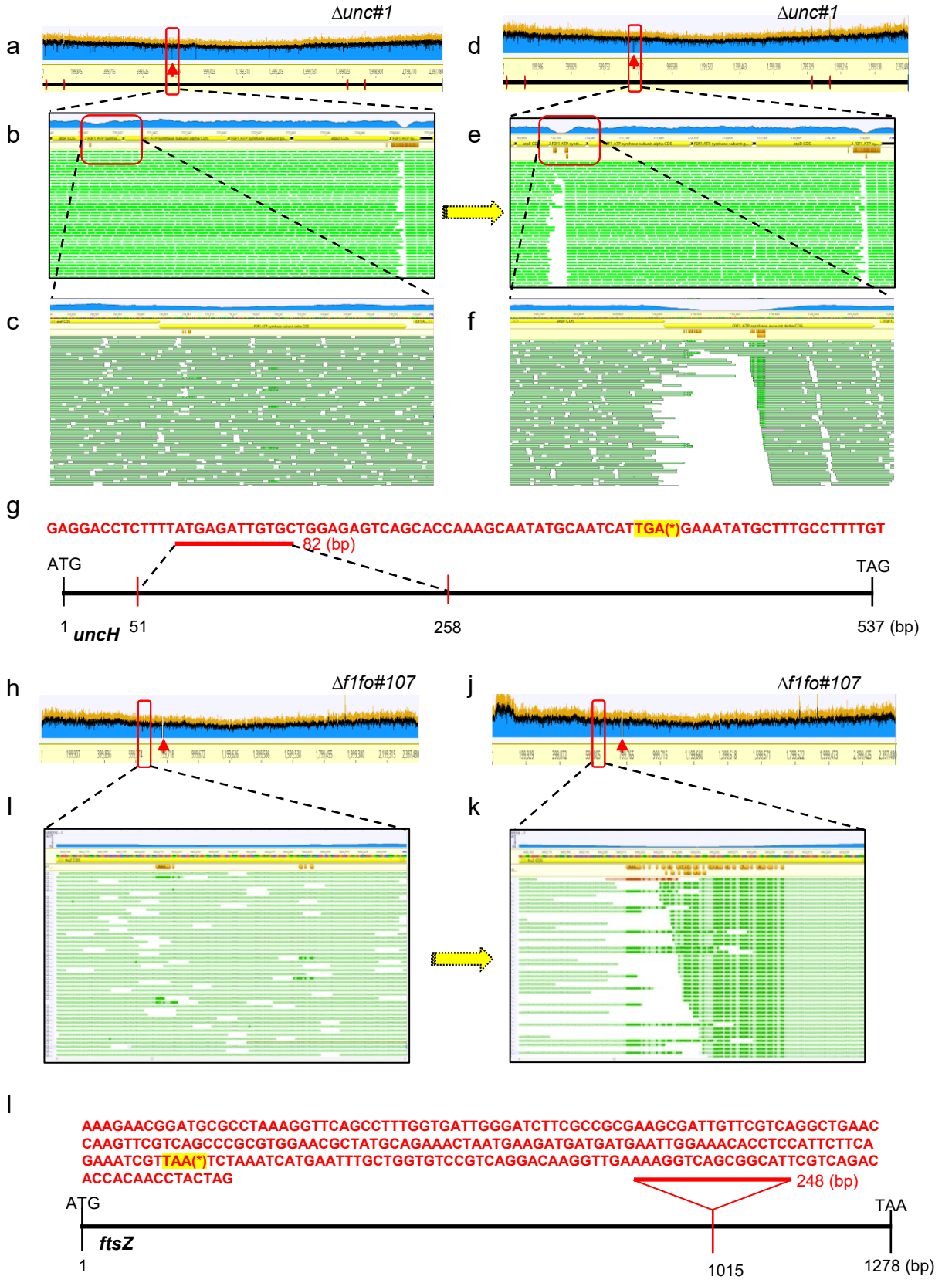
Δunc#1
a
b
c
d
e
f
g
GAGGACCTCTTTTATGAGATTGTGCTGGAGAGTCAGCACCAAAGCAATATGCAATCATTGA(*)GAAATATGCTTTGCCTTTTGT
82 (bp)
ATG
TAG
1
uncH
51
258
537 (bp)
Δf1fo#107
h
j
l
k
l
AAAGAACGGATGCGCCTAAAGGTTCAGCCTTTGGTGATTGGGATCTTCGCCGCGAAGCGATTGTTCGTCAGGCTGAAC
CAAGTTCGTCAGCCCGCGTGGAACGCTATGCAGAAACTAATGAAGATGATGATGAATTGGAAACACCTCCATTCTTCA
GAAATCGTTAA(*)TCTAAATCATGAATTTGCTGGTGTCCGTCAGGACAAGGTTGAAAAGGTCAGCGGCATTCGTCAGAC
ACCACAACCTACTAG
248 (bp)
ATG
TAA
ftsZ
1
1015
1278 (bp)

Fig S6

a

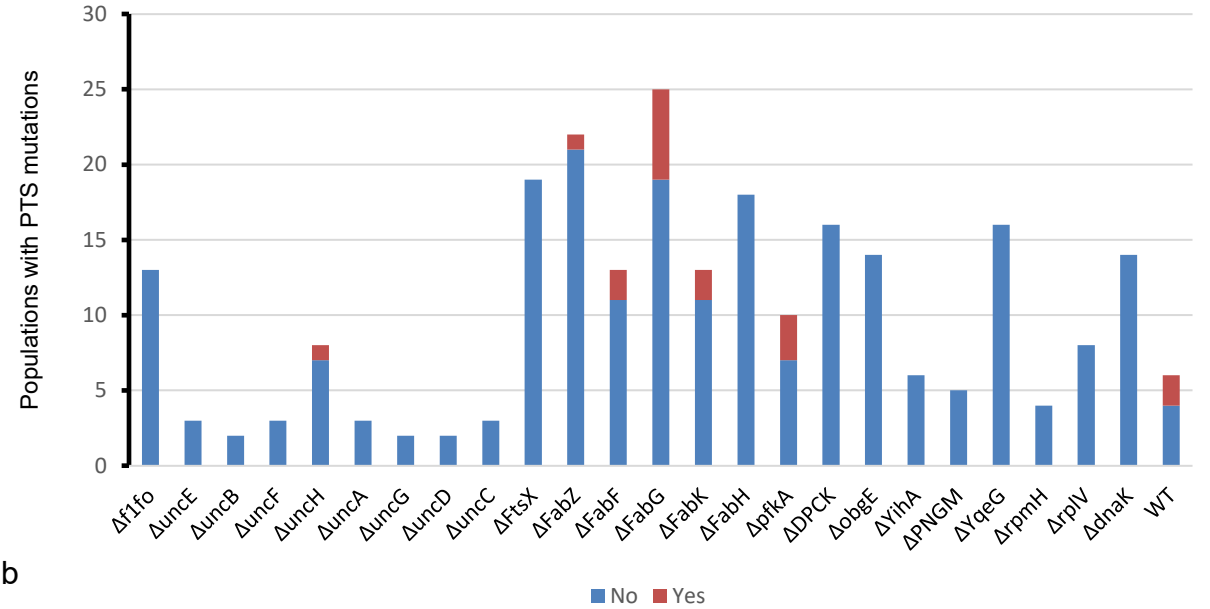
Populations with PTS mutations
30
25
20
15
10
5
0
Δf1fo
ΔuncE
ΔuncB
ΔuncF
ΔuncH
ΔuncA
ΔuncG
ΔuncD
ΔuncC
ΔFtsX
ΔFabZ
ΔFabF
ΔFabG
ΔFabK
ΔFabH
ΔpfkA
ΔDPCK
ΔobgE
ΔYihA
ΔPNGM
ΔYqeG
ΔrpmH
ΔrplV
ΔdnaK
WT
No
Yes

b

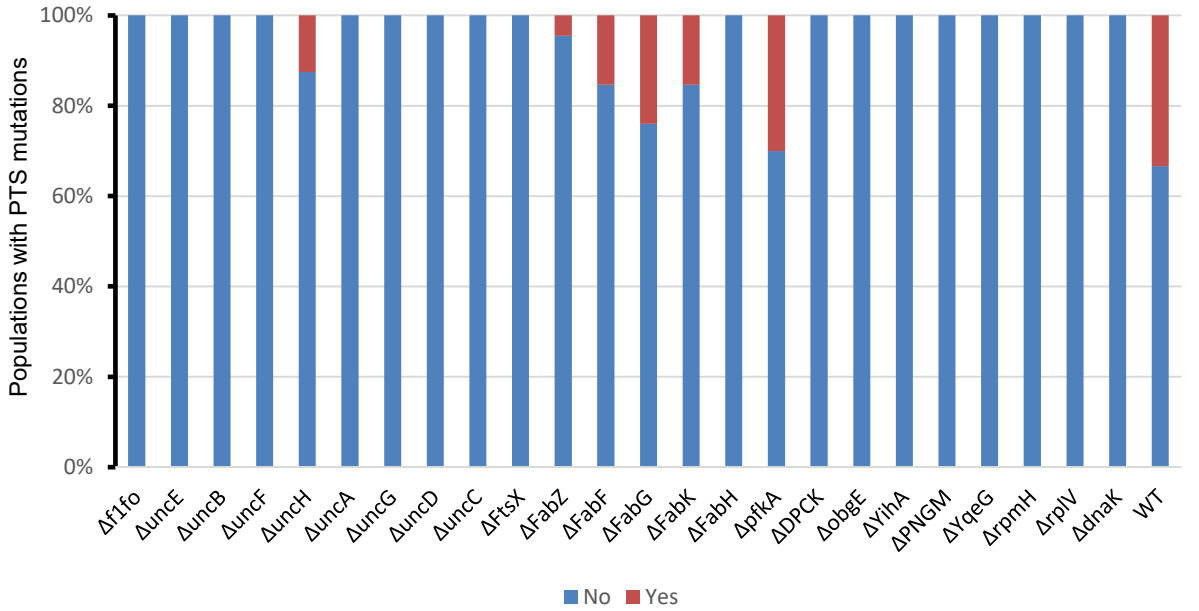
Populations with PTS mutations
100%
80%
60%
40%
20%
0%
Δf1fo
ΔuncE
ΔuncB
ΔuncF
ΔuncH
ΔuncA
ΔuncG
ΔuncD
ΔuncC
ΔFtsX
ΔFabZ
ΔFabF
ΔFabG
ΔFabK
ΔFabH
ΔpfkA
ΔDPCK
ΔobgE
ΔYihA
ΔPNGM
ΔYqeG
ΔrpmH
ΔrplV
ΔdnaK
WT
No
Yes

Fig S7

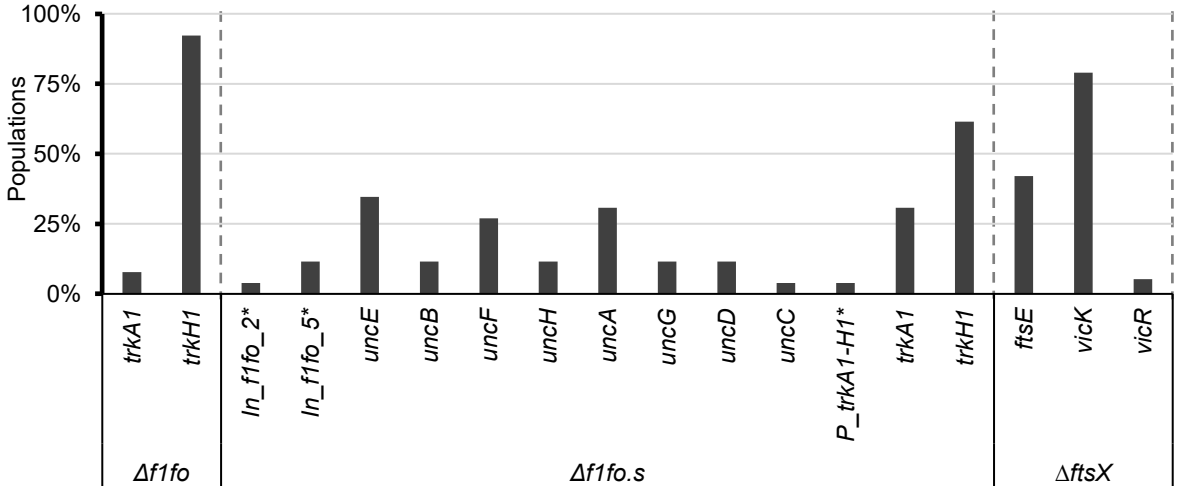
100%
75%
50%
25%
0%
Populations
trkA1
trkH1
In_f1fo_2*
In_f1fo_5*
uncE
uncB
uncF
uncH
uncA
uncG
uncD
uncC
P_trkA1-H1*
trkA1
trkH1
ftsE
vicK
vicR
Δf1fo
Δf1fo.s
ΔftsX

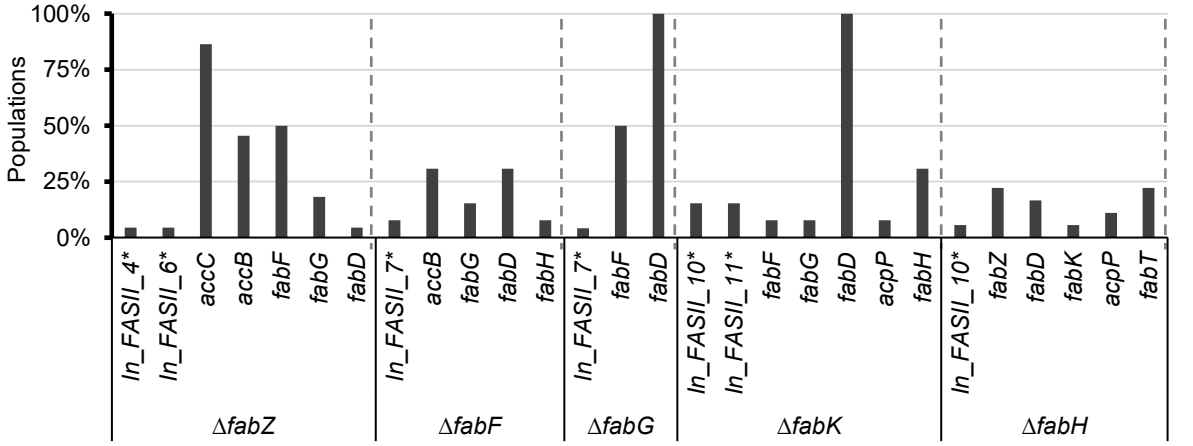
100%
75%
50%
25%
0%
Populations
In_FASII_4*
In_FASII_6*
accC
accB
fabF
fabG
fabD
In_FASII_7*
accB
fabG
fabD
fabH
In_FASII_7*
fabF
fabD
In_FASII_10*
In_FASII_11*
fabF
fabG
fabD
acpP
fabH
In_FASII_10*
fabZ
fabD
fabK
acpP
fabT
ΔfabZ
ΔfabF
ΔfabG
ΔfabK
ΔfabH

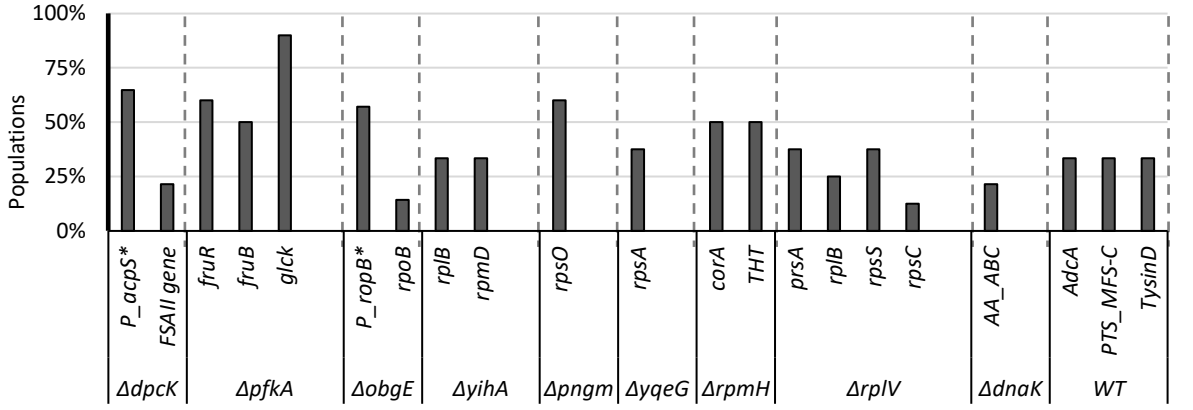
100%
75%
50%
25%
0%
Populations
P_acpS*
FSAII gene
fruR
fruB
glck
P_ropB*
rpoB
rplB
rpmD
rpsO
rpsA
corA
THT
prsA
rplB
rpsS
rpsC
AA_ABC
AdcA
PTS_MFS-C
TysinD
ΔdpcK
ΔpfkA
ΔobgE
ΔyihA
Δpngm
ΔyqeG
ΔrpmH
ΔrplV
ΔdnaK
WT

Fig S8

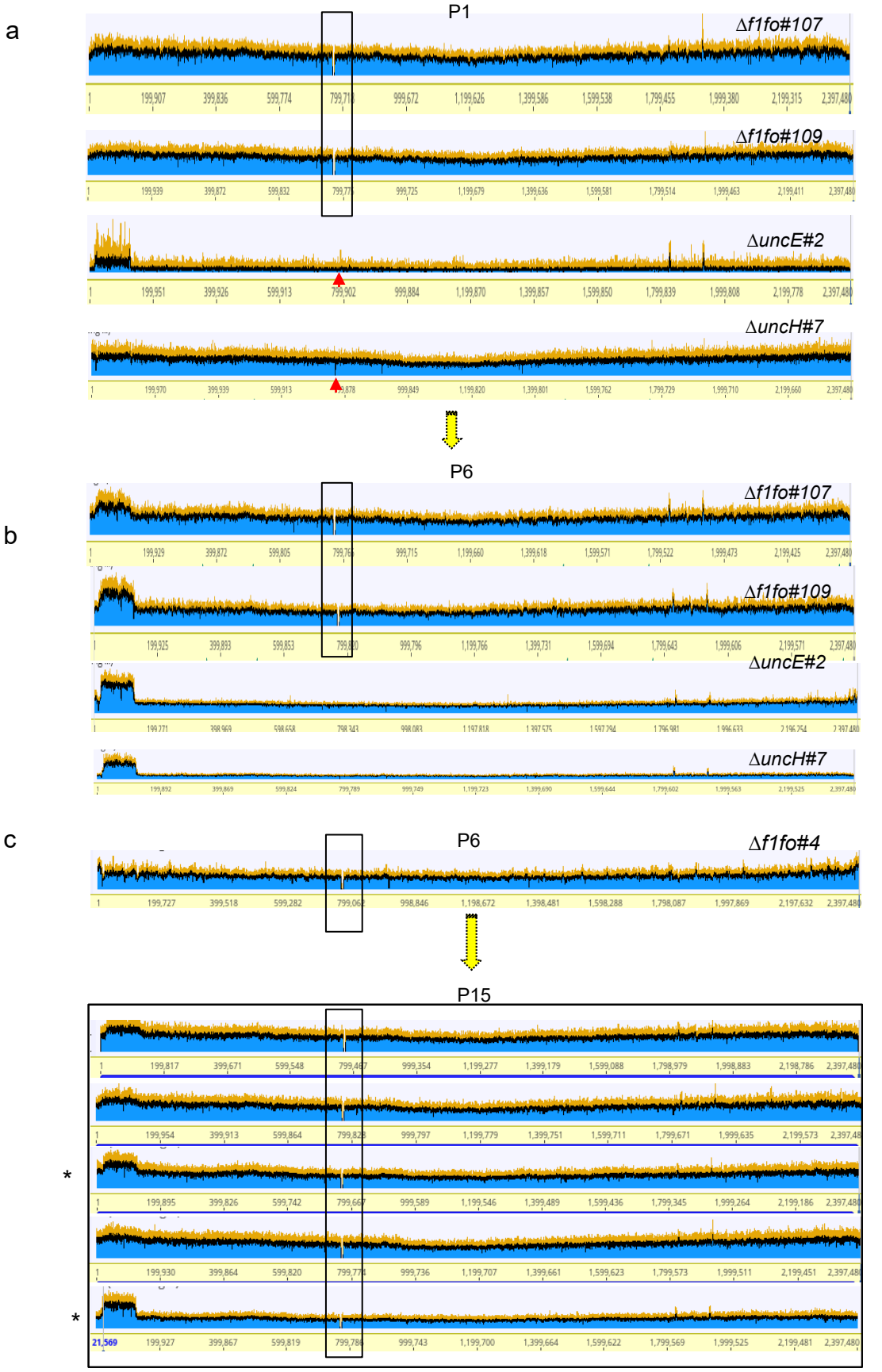
a
P1
Δf1fo#107
Δf1fo#109
ΔuncE#2
ΔuncH#7
b
P6
Δf1fo#107
Δf1fo#109
ΔuncE#2
ΔuncH#7
c
P6
Δf1fo#4
P15
*
*

Fig S9

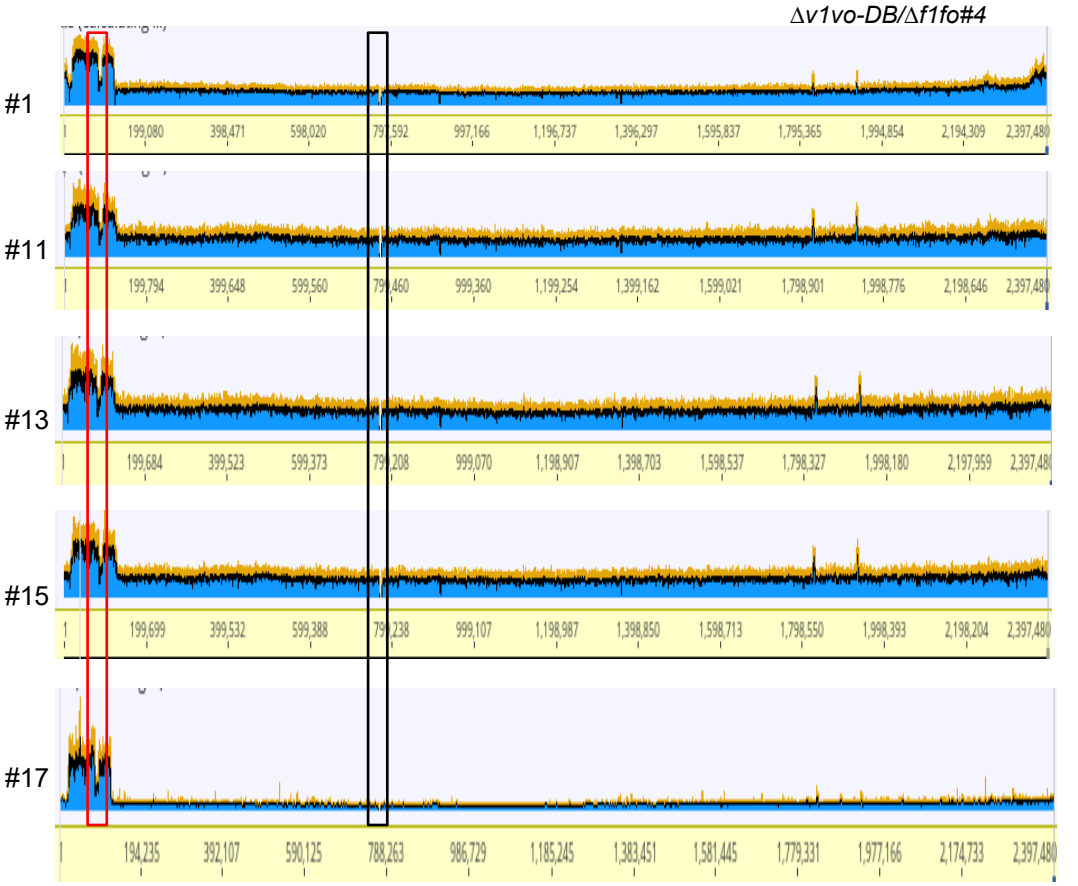
Δv1vo-DB/Δf1fo#4
#1
199,080
398,471
598,020
997,166
1,196,737
1,396,297
1,595,837
1,795,365
1,994,854
2,194,309
#11
199,794
399,648
599,560
999,360
1,199,254
1,399,162
1,599,021
1,798,901
1,998,776
2,198,646
#13
199,684
399,523
599,373
999,070
1,198,907
1,398,703
1,598,537
1,798,327
1,998,180
2,197,959
#15
199,699
399,532
599,388
999,107
1,198,987
1,398,850
1,598,713
1,798,550
1,998,393
2,198,204
#17
194,235
392,107
590,125
788,263
986,729
1,185,245
1,383,451
1,581,445
1,779,331
1,977,166
2,174,733

Fig S10

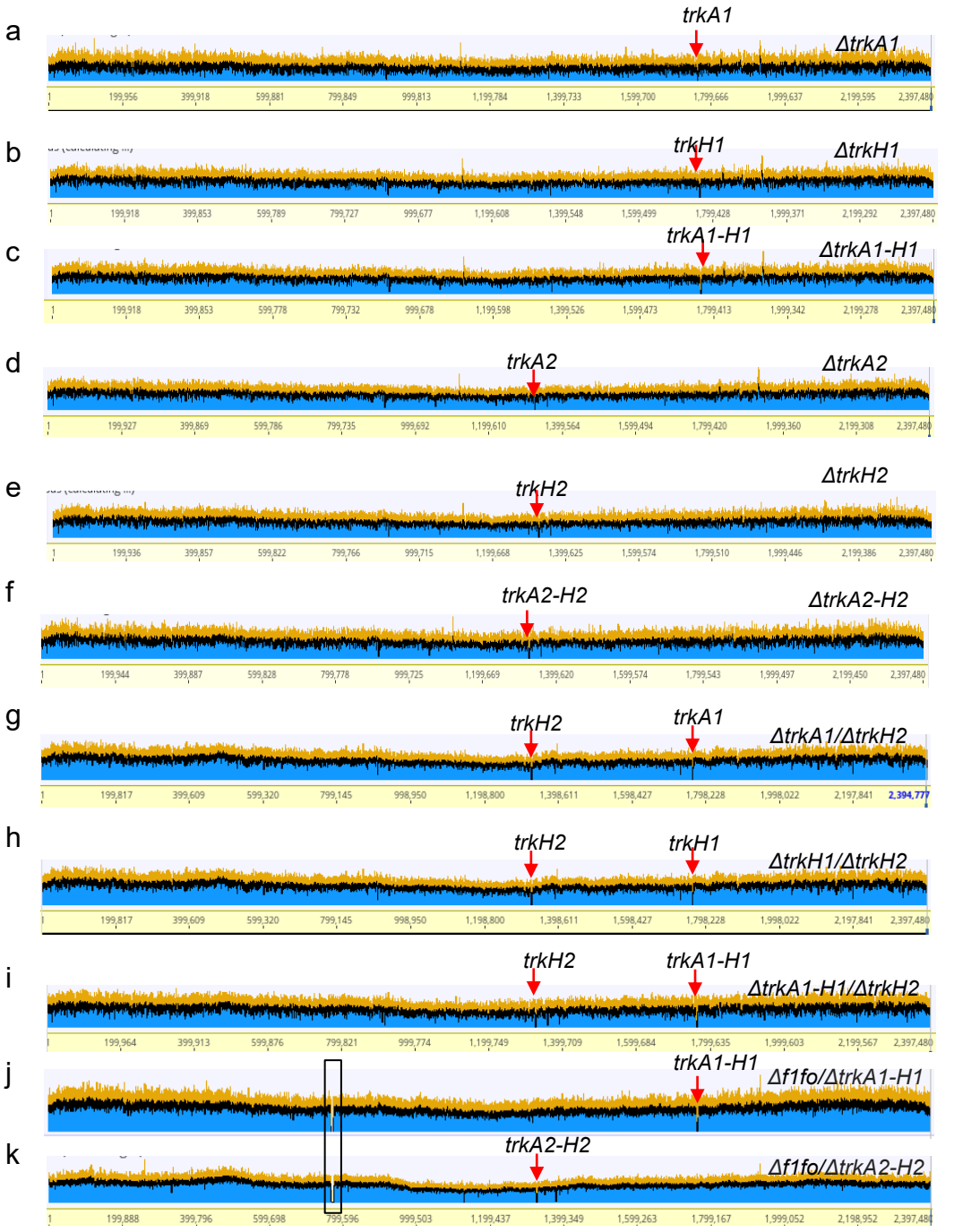
a
trkA1
ΔtrkA1
b
trkH1
ΔtrkH1
c
trkA1-H1
ΔtrkA1-H1
d
trkA2
ΔtrkA2
e
trkH2
ΔtrkH2
f
trkA2-H2
ΔtrkA2-H2
g
trkH2
trkA1
ΔtrkA1/ΔtrkH2
h
trkH2
trkH1
ΔtrkH1/ΔtrkH2
i
trkH2
trkA1-H1
ΔtrkA1-H1/ΔtrkH2
j
trkA1-H1
Δf1fo/ΔtrkA1-H1
k
trkA2-H2
Δf1fo/ΔtrkA2-H2

Fig S11 Working model for F1Fo, V1Vo, TrkA1-H1 and TrkA2-H2

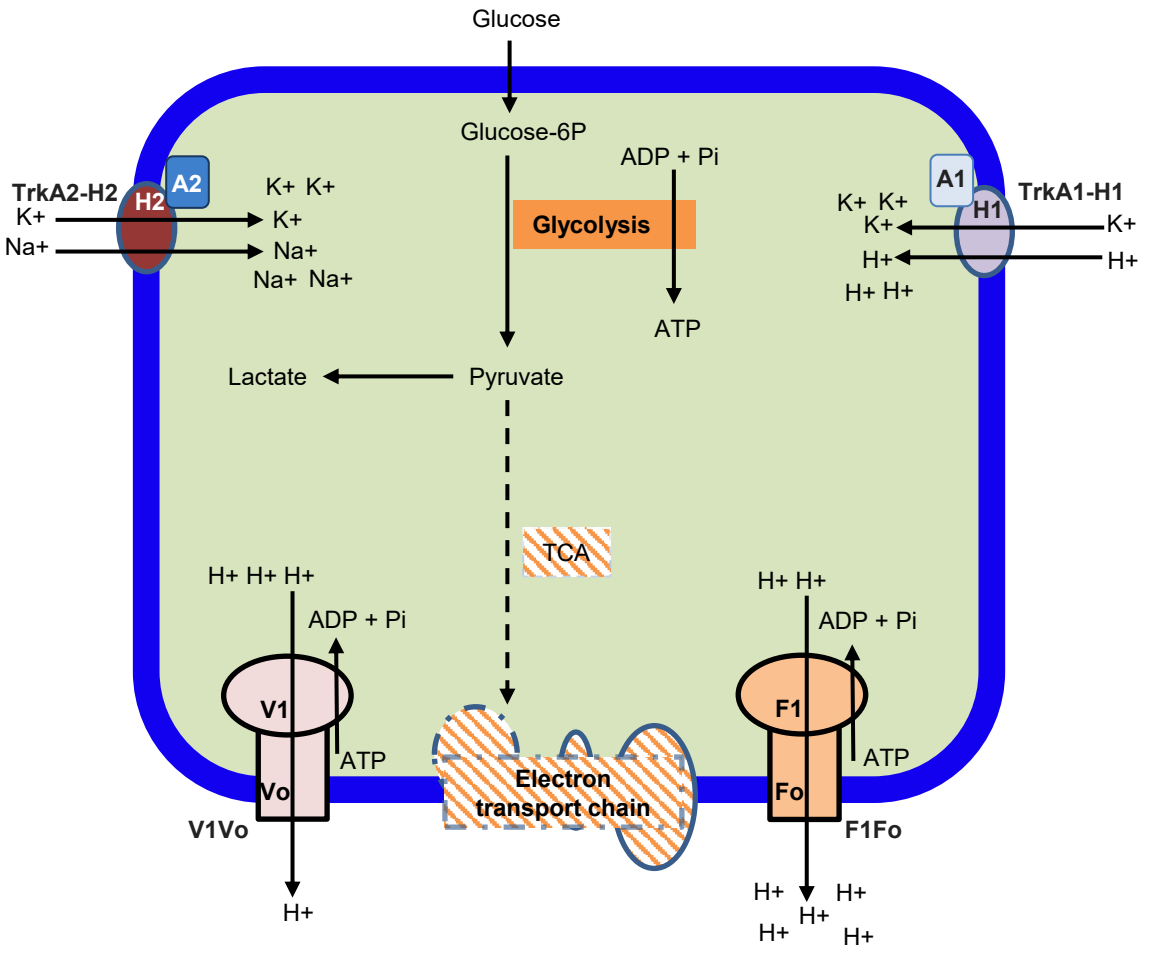

Fig S12

a

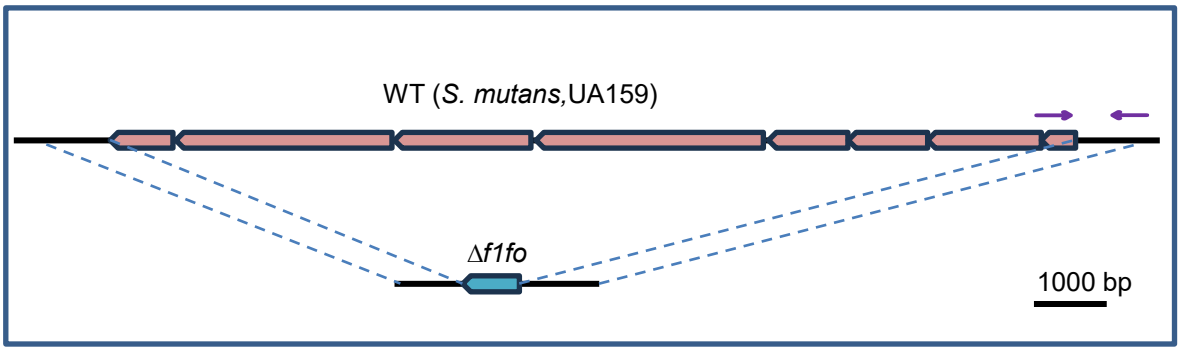

b

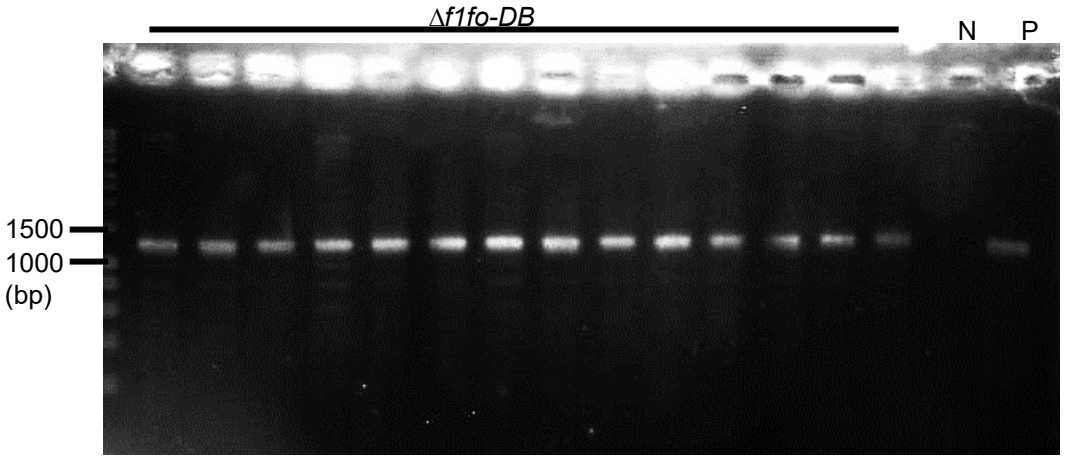

Fig S13

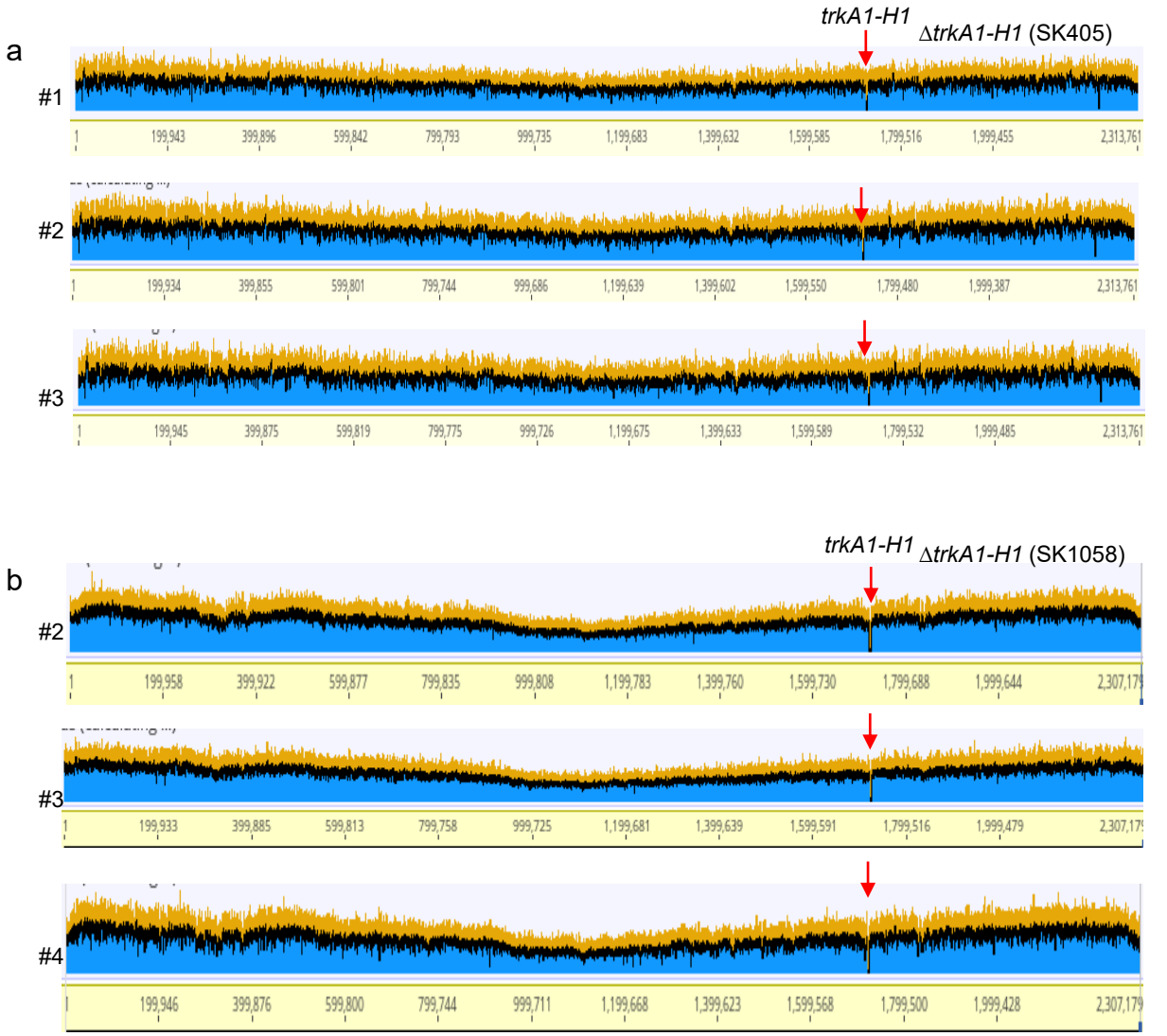
a
trkA1-H1
ΔtrkA1-H1 (SK405)
#1
1
199,943
399,896
599,842
799,793
999,735
1,199,683
1,399,632
1,599,585
1,799,516
1,999,455
2,313,761
#2
1
199,934
399,855
599,801
799,744
999,686
1,199,639
1,399,602
1,599,550
1,799,480
1,999,387
2,313,761
#3
1
199,945
399,875
599,819
799,775
999,726
1,199,675
1,399,633
1,599,589
1,799,532
1,999,485
2,313,761
b
trkA1-H1
ΔtrkA1-H1 (SK1058)
#2
1
199,958
399,922
599,877
799,835
999,808
1,199,783
1,399,760
1,599,730
1,799,688
1,999,644
#3
1
199,933
399,885
599,813
799,758
999,725
1,199,681
1,399,639
1,599,591
1,799,516
1,999,479
#4
1
199,946
399,876
599,800
799,744
999,711
1,199,668
1,399,623
1,599,568
1,799,500
1,999,428

Fig S14

a

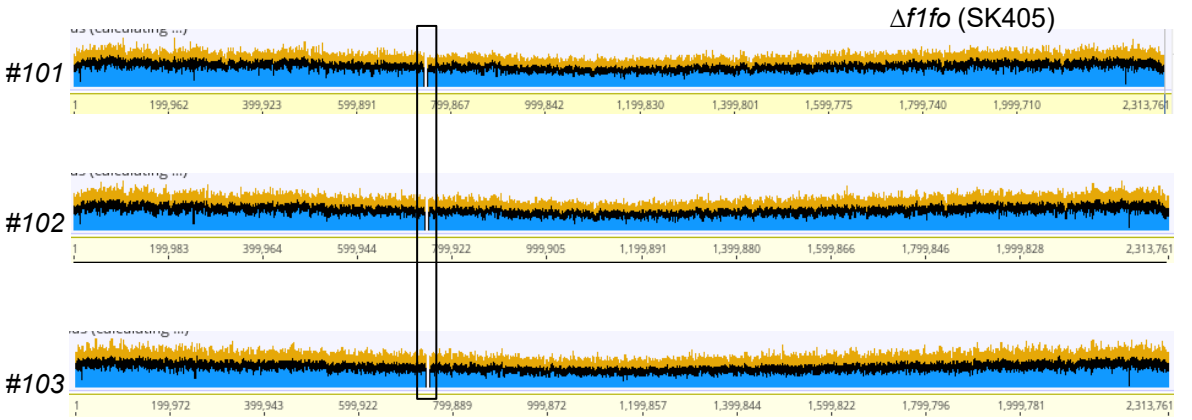
Δf1fo (SK405)
#101
1
199,962
399,923
599,891
799,867
999,842
1,199,830
1,399,801
1,599,775
1,799,740
1,999,710
2,313,761
#102
1
199,983
399,964
599,944
799,922
999,905
1,199,891
1,399,880
1,599,866
1,799,846
1,999,828
2,313,761
#103
1
199,972
399,943
599,922
799,889
999,872
1,199,857
1,399,844
1,599,822
1,799,796
1,999,781
2,313,761

b

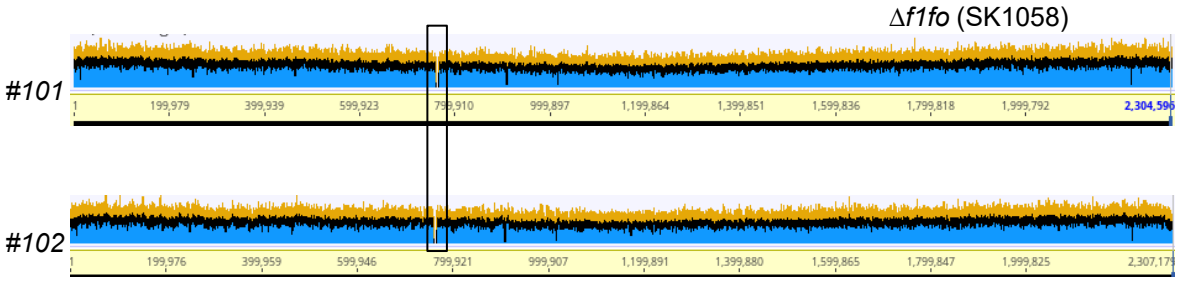
Δf1fo (SK1058)
#101
1
199,979
399,939
599,923
799,910
999,897
1,199,864
1,399,851
1,599,836
1,799,818
1,999,792
2,304,596
#102
1
199,976
399,959
599,946
799,921
999,907
1,199,891
1,399,880
1,599,865
1,799,847
1,999,825
2,307,179